KWRRI Research Reports

Kentucky Water Resources Research Institute

1988

Predicting Potential Aluminum Contamination of Surface and Ground Waters from Acid Sulfate Enriched Drainages Emanating from Low Neutralization Capacity Watersheds

Anastasios D. Karathanasis
University of Kentucky, akaratha@uky.edu

Vasilios P. Evangelou
University of Kentucky

Y. L. Thompson
University of Kentucky

PREDICTING POTENTIAL ALUMINUM CONTAMINATION OF SURFACE AND GROUND WATERS FROM ACID SULFATE ENRICHED DRAINAGES EMANATING FROM LOW NEUTRALIZATION CAPACITY WATERSHEDS

BY

A.D. Karathanasis
V.P. Evangelou

Principal Investigators

Y.L. Thompson

Research Assistant

1988

PREDICTING POTENTIAL ALUMINUM CONTAMINATION OF SURFACE AND GROUND WATERS FROM ACID SULFATE ENRICHED DRAINAGES EMANATING FROM LOW NEUTRALIZATION CAPACITY WATERSHEDS

By

A.D. Karathanasis
V.P. Evangelou

Principal Investigators

Y.L. Thompson

Research Assistant

DISCLAIMER

Contents of this report do not necessarily reflect the views and policies of the United States Department of the Interior, Washington, D.C., nor does mention of trade names or commerical products constitute their endorsement or recommendation for use by the U.S. Government.

ABSTRACT

The composition of soil solutions and surface waters emanating from unreclaimed, or partially reclaimed, strip-mined watersheds with low buffering capacity in Kentucky were compared with soil solution compositions of unaffected strata in the watershed. The data suggest that almost 20 years after mining, most soil solutions and surface waters of the disturbed areas still contain high levels of dissolved Al, controlled primarily by the solubilities of a jurbanite-like mineral (upper limit) and alunite (lower limit). Soluble Al in solutions of undisturbed areas was consistent with the solubility of kaolinite or gibbsite. The absence of jurbanite x-ray diffraction peaks suggested the presence of an amorphous mineral or one stoichiometrically similar to jurbanite. Despite greater residence times for soil solutions as compared to surface waters, their compositional differences were insignificant. The control of soluble Al by basic aluminum sulfate minerals was not affected by the variable mineralogical and textural composition of soil and geologic strata in the watershed. Apparently, this is the result of low buffering capacity. At pH < 4, pH and sulfate activities can be used to accurately predict the levels of soluble Al^{3+} in surface and ground waters of the watersheds. Similar predictions from pH and SO_4^{2-} activities can also be made for dissolved Fe^{3+} levels, supporting the stoichiometry but a much higher solubility than that of jarosite.

Column leaching experiments of selected spoil, soil and sediment samples contaminated by acid mine drainage over a period of five months also confirmed that pH, SO_4^{2-}, Al and Fe are the major components controlling the behavior of these systems. Alternating wetting and drying cycles appeared to cause more drastic changes in the above components than different flow rates simulating rain events of different intensity. Kinetic profiles of Al and Fe released from the studied materials suggested that at different stages of leaching these materials may be releasing different levels of Al and Fe controlled by the solubility of characteristic sequences of basic Al-sulfate, Al-hydroxide and aluminosilicate minerals or Fe-sulfate, Fe-hydroxide minerals, which are watershed specific. The jurbanite-jurbanite, jurbanite-alunite and the jurbanite-alunite-microcrystalline gibbsite appeared to be the dominant sequences controlling the solubility of Al. Similarly, the jarosite-amorphous Fe (OH_3) or amorphous $Fe(OH_3)$- goethite sequence appeared to control

the solubility of Fe. These findings suggest that equilibrium relationships, although quite useful, may not be sufficient for predicting the dynamic behavior of systems such as those included in this study. Kinetic relationships which reflect Al and Fe released as a function of time and the sequence of mineral phases controlling Al and Fe solubility are also necessary in order to obtain more realistic models of Al and Fe release into aquifers of such systems.

Descriptors:

      Dissolved Aluminum, Aluminum Sulfates, Water Flow Rates, Mineral Equilibria, Acid Soils.

TABLE OF CONTENTS

PART I

ALUMINUM AND IRON EQUILIBRIA

IN SOIL SOLUTIONS AND SURFACE WATERS

PART I

INTRODUCTION

High concentrations of dissolved Al are typical in acid drainages running off or percolating through soil and geological strata of surface mined watersheds (Bieseker and George, 1966; Van Breemen, 1973; Rogowski et al., 1977; Caruccio and Geidel, 1978; Nordstrom, 1982;). There is insufficient evidence that Al is toxic to fauna or humans, but high Al levels in acidified lakes cause reduced fish populations (Baker and Schofield, 1982).

In most naturally acidified terrestrial or aquatic environments soluble Al is assumed to be controlled by the solubility of gibbsite or kaolinite. However, most acid mine drainages are sulfate-rich solutions acidified by pyrite oxidation. The aqueous geochemistry of Al is modified considerably in such sulfate systems (Nordstrom, 1982). Gibbsite and kaolinite no longer dictate Al levels in solution; rather Al levels are controlled by newly precipitating basic Al-sulfate minerals (Van Breemen, 1973; Nordstrom, 1982; Anthony and McLean, 1976; Evangelou and Karathanasis, 1984). The nature and solubility of basic aluminum sulfates vary with soil pH and the physicochemical and mineralogical characteristics of soil and geologic strata in the watershed (Singh and Brydon, 1969; Frink, 1973; Adams and Hajek, 1978; SSSA, 1982; Driscoll et al., 1984; Rodriguez and Hidalgo, 1985; Nordstrom and Ball, 1986). For pH values < 4.5, surface mine drainages frequently appear to be undersaturated with respect to gibbsite and kaolinite, and their Al concentrations appear to be related to the solubilities of the aluminum sulfate minerals alunite, jurbanite and basaluminte (Nordstrom, 1982). These minerals are less soluble than gibbsite or kaolinite and can dramatically modify the upper limits of dissolved Al in surface and ground waters of acid mine drainage inflicted watersheds (Van Breemen, 1973; Nordstrom, 1982; Evangelou and Karathanasis, 1984). Aluminum concentrations in solutions reaching the aquifer are expected to be especially high in watersheds dominated by sandstone, shale and siltstone geologic strata which lack the neutralization capacity of limestone beds (Biesecker and George, 1966).

The equilibrium of Fe is also significantly modified in an acid sulfate system (Van Breemen and Harmsen, 1975; Nordstrom et al., 1979, SSSA, 1982). While goethite or amorphous $Fe(OH)_3$ control Fe levels in most natural aquatic

2

systems (Stumm and Morgan, 1981), dissolved Fe in acid sulfate-rich solutions appears to be more consistent with the solubility of the basic iron sulfate mineral jarosite. This mineral, however, is metastable and gradually transforms under field conditions to the more stable goethite or hematite (Van Breemen and Harmsen, 1975).

The research objectives of this study were:

1. To identify and characterize indigenous and newly precipitated stable Al and Fe minerals, forming through acid sulfate drainage - soil interactions, likely to control the solubility of Al and Fe in effluents of runoff and infiltration waters of watersheds with diverse mineralogical composition.

2. To determine the role of clay-colloids present in specific low neutralization capacity soil or geologic systems in modifying the composition of water solutions emanating from acid sulfate drainage inflicted watersheds.

3. To establish empirical relationships defining and predicting potential levels of Al and Fe released in water reservoirs by acid sulfate drainage contaminated soils and geologic strata of specific geographic regions of Kentucky.

Although the solubility product-equilibrium approach used in these watersheds presents several inherent limitations (the systems are heterogenous, non-equilibrium, and open), comparisons between predicted equilibrium compositions and actual solution compositions should be useful in better understanding the Al and Fe physicochemical behavior of the watersheds.

MATERIALS AND METHODS

The study sites designated as OH, BD, and CL were located in Ohio, Boyd, and Clinton Counties of Kentucky, respectively. The watersheds were chosen to represent different geological strata, major mineable coal seams, and soils with low neutralization capacity (absence of carbonates) in western (OH), eastern (BD) and southern (CL) areas of the Kentucky coal fields. Site characteristics and descriptions of the collected samples are given in Tables 1 and 2. All watersheds were mined prior to 1973 and were subjected to little or no reclamation. Twelve undisturbed soil and sediment samples contaminated by acid mine drainage, 10 spoil samples, and 8 undisturbed, uncontaminated soil and sediment samples were collected in October of 1986. Eleven surface water samples from seeps, sedimentation ponds and streams were also collected from the same watersheds. Soil and sediment samples were collected with their natural moisture and sealed in polyethylene bags. Thereafter, the samples were uniformly saturated with sufficient deionized water to approach their water holding capacities and left undisturbed in a controlled temperature (25°C) storage chamber for 90 days. Following the equilibration period, interstitial soil solutions were extracted by centrifugation and filtered through a 0.45 μm membrane filter. Extracts were analyzed in duplicate for pH, Al, Fe, Ca, Mg, K, Na, Mn, Si, S, and Cl. Surface water samples were analyzed similarly within a week after sampling. Iron, Ca, Mg, K, Na and Mn were determined by atomic absorption using an Instrumentation Laboratory S-11 spectrometer. Aluminum and Si were determined colorimetrically using the eriochrome cyanine-R_2, and the amino acid-reduced molybdosilicic blue method (APHA, 1976), respectively; sulfate - S was measured turbidimetrically, and Cl titrimetrically, using standard methods (American Public Health Association, 1976).

Following extraction, soil, sediment, and spoil subsamples were air-dried, gently crushed to pass a 2 mm sieve, and analyzed for particle size distribution, pH, extractable bases, CEC (SCS, 1982) and mineralogy of the whole-soil and the < 2 μm clay fraction (Karathanasis and Hajek, 1982). Whole-soil mineralogical analysis was performed on powder samples by x-ray diffraction (XRD). Mineral quantities were estimated from peak areas of XRD and thermogravimetry (TG) using an 1840 Philips Cu-Kα diffractometer and a Dupont 1090 Thermal Analyzer, respectively (Karathanasis and Hajek, 1982).

Solution ionic activities were calculated by using the extended Debye-Huckel equation and a method of successive approximations (Adams, 1971), which included the following ion pairs: $CaSO_4^0$, $MgSO_4^0$, KSO_4^-, $NaSO_4^-$, $CaHPO_4^0$, $MgHPO_4^0$, $AlSO_4^+$, and $FeSO_4^+$. Solution Al was distributed among the following species: $Al(OH)^{2+}$, $Al(OH)_2^+$, $Al(OH)_3^0$, and $AlSO_4^+$, using dissociation constants from Adams (1971), and May et al. (1979) (Table 3). All solutions had negligible or non-detectable levels of P, F and dissolved organic carbon. Iron (Fe^{3+}) activity in solution was calculated from total Fe distribution into ionic species similar to those used for Al speciation, plus Fe^{2+}, which was determined by the orthophenanthroline method (APHA 1976). The dissociation constants used for Fe speciation were taken from Lindsay (1979) (Table 3).

RESULTS AND DISCUSSION

Physicochemical and Mineralogical Characteristics

Particle size distributions, soil pH, extractable bases and cation exchange capacity (CEC) of the samples studied are reported in Table 4. The samples covered a wide textural range representing loamy sand, sandy loam, loam, silt loam, silty clay loam, clay loam, sandy clay loam, silty clay and clay textures. The pH of the contaminated soil/spoil/sediment samples ranged from 3.20 to 4.27 with an average value of about 3.7. The uncontaminated samples had a pH range of 4.37 to 6.06 with the highest pH's (CL-1A and CL-1B samples) being the result of the buffering capacity of underlying limestone beds at the base of the watershed. The extractable base distributions in most contaminated samples favored Mg over Ca. Uncontaminated samples showed the opposite trend. Based on comparisons between CEC and total extractable bases, Al appeared to be the dominant saturating cation of the exchange phase in most samples. The relatively high CEC's of samples OH-1B, OH-1D, and OH-1E are the result of high clay content or presence of montmorillonite in the clay fraction. These samples were the only ones to contain considerable amounts of minerals with high buffering capacity (montmorillonite, vermiculite).

Mineralogical compositions of whole soil (< 2 mm) and clay (< 2 μm) fractions are reported in Tables 5 and 6, respectively. Of the aluminosilicate minerals, kaolinite was the dominant mineral in the clay fraction of all but one sample (BD-3A), in which mica predominated. Kaolinite was also the second most dominant mineral after quartz in most whole soil samples, except those high in jarosite. Mica was in general the next most abundant aluminosilicate of whole soil samples followed closely by feldspars. Vermiculite (OH1, OH2, BD) and 1.0/1.4 nm interstratified minerals (OH1, OH2) were also found in minor quantities. In addition to the OH-1B, OH-1D, and OH-1E samples, three other samples from the OH-1, OH-2 watersheds, two from the BD and four from the CL watershed also contained some smectite or vermiculite in their clay fraction. Clay size mica was within the same range as in whole soil samples. Other silicate minerals in small quantities included HIV (high in CL-1A and CL-1B), 1.0/1.4 nm interstratified, quartz, and feldspars. Goethite was common in most samples while gibbsite was detected only in samples OH-2E and CL-1A.

6

Aluminum sulfate minerals were detected in small to moderate quantities primarily in the whole soil fraction of most of the contaminated samples. Alunite and aluminite were most common with sporadic appearances by basaluminite and hydrobasaluminite. Of the other sulfate minerals, jarosite was the most frequent encounter with sporadic appearances by gypsum and anhydrite. The high concentrations of jarosite and alunite in some clay fractions are indicative of fairly good crystallinity. On the other hand, the absence of jurbanite XRD peaks in all samples, in spite of support from solution compositions, suggests a very poorly crystalline component. The latter discrepancy, which appears to be common in acid mine drainage environments, prompted Van Breemen (1973) to call jurbanite a "mystery mineral".

Soil Solution and Surface Water Composition

Elemental and ionic composition of soil solutions and surface waters are listed in Tables 7, 7a, 8 and 8a, respectively. Solution and water pH values were generally considerably lower than soil pH's, ranging from 1.96 to 3.96 in contaminated samples. Solution pH values of uncontaminated samples, although lower, were closer to their respective soil pH. The pH of surface waters agreed fairly well (some waters had slightly higher pH) with the pH of interstitial soil solutions percolating through the spoil, sediment or soil strata of the watershed. There was no consistent relationship between amount of clay or type of mineralogy and the pH of soil solutions or surface waters in the watershed. This indicates that the low buffering capacity of these materials has already been consumed by the chemistry of the acid mine drainage waters.

The highest Al concentrations were found in the OH1 and OH2 watersheds. The water sample collected from the flume of the CL watershed had no detectable Al. Generally, surface waters contained lower Al concentrations than percolating soil solutions and the Al concentrations decreased with distance from the disturbed area. This trend is best illustrated in the BD watershed where the flume water sample (BD-7) at the base of the watershed contains only 0.23 mM Al while samples BD-8 and BD-9 representing drainages of increasing proximity to the disturbed area contain 0.66 and 0.71 mM Al, respectively. Similar trends were observed in all watersheds. Again, as with

7

the pH, there was no evidence of buffering of the amounts of Al released in the watersheds by increases in clay content or presence of high charge minerals. The reduced Al concentrations found in surface waters, versus those found in percolating waters of comparable pH levels are attributed to dilution effects and precipitation of aluminum sulfate minerals, which remove considerable amounts of Al from the drainage water. Aluminum sulfate precipitation is supported by mineralogical and solution composition data as well as by the good correlation ($r = 0.92$) between Al and SO_4 concentrations. The high Si concentrations of most solutions and surface waters (compared to the solubility of quartz) verify that their high Al level is the product of extensive destruction of aluminosilicate minerals from the interaction between acid mine drainage and spoil/soil/sediment strata. The relatively good agreement between total Fe and SO_4 concentrations also suggested a possible control of soluble Fe by iron sulfate minerals especially in solutions with high iron concentrations. This was supported by mineralogical data indicating small to moderate amounts of jarosite in several contaminated samples. The low Fe and SO_4 content of uncontaminated soil solutions and some surface waters suggests Fe-control by a sulfate-free Fe mineral (Fe-hydroxide or Fe-hydroxyoxide).

From the other solution components the higher Na levels over those of K are attributed to the abundance of albite versus orthoclase (confirmed by XRD) and the lower interaction of Na as compared to that of K with the solid phase. Calcium, Mg, and sulfate concentrations, although high, are within the expected range for acid sulfate weathering materials. Calcium concentrations were generally close to the range supported by the solubility of gypsum, especially in the OH watersheds.

Mineral Phase Regulation of Aluminum Levels

Solution ionic activities were used to assess the potential equilibrium of Al^{3+} in soil solutions and surface waters with mineral phases. Mineral phases that were evaluated included gibbsite (poorly and well crystalline with pK's of 32.4 and 33.9, respectively), kaolinite (pK = 76.4), alunite ($KAl_3(SO_4)_2(OH)_6$; pK = 85.4), jurbanite ($Al(SO_4)(OH).5H_2O$; pK = 3.8) and basaluminite ($Al_4(SO_4)(OH)_{10}.5H_2O$: pK = 117.6).

A plot of pH versus the negative logarithm of the activity of Al^{3+} in Fig. 1 suggests at least two possible controls of Al equilibrium in solutions with pH < 4.2 and those with pH > 4.2. Although the break in slope may cover the pH range from 4.2 to 5.0, it is apparent that the activity of Al^{3+} in solutions and surface waters of low pH (< 4.2) is consistent with the stoichiometry of jurbanite and those of pH > 4.2 with the solubility of kaolinite or gibbsite. These trends are in agreement with data reported by Nordstrom and Ball (1986), indicating a slope break in the pH range of 4.5 to 5.0 as the separation boundary for Al^{3+} control between basic aluminum sulfates and aluminosilicates. This suggests that Al^{3+} levels in all solutions in contact with contaminated samples and surface waters are controlled primarily by the solubility of basic aluminum sulfate minerals since their pH is < 4.2. On the other hand, Al^{3+} in solutions of uncontaminated soils is controlled by aluminosilicate minerals.

Although surface waters, because of their shorter residence time, should exhibit increasing tendencies toward mineral saturation with aluminosilicates rather than basic aluminum sulfate minerals, no such trend was detected in the watersheds studied. The only exception was the water sample collected from the flume of the CL watershed located below Mississippian limestone beds. This sample had undetectable amounts of Al and therefore it is not plotted in Fig. 1.

The control of Al^{3+} activities in soil solutions and surface waters of the contaminated watersheds by basic aluminum sulfate minerals is also illustrated in Fig. 2. The positive slope of this regression line (1.3) agrees very well with that reported by Nordstrom and Ball (1986) for acid mine waters of California and is explained by the conservative SO_4^{2-} behavior attributed to dilution factors. A plot of Al^{3+} activities versus pH + pSO_4 in Fig. 3 leaves no doubt that solution Al^{3+} is controlled by the solubility of an aluminum sulfate mineral with 1:1:1 ($Al:SO_4:OH$) stoichiometry. The excellent fit of the data to this regression line suggests that pH and SO_4^{2-} activities can predict with 85% accuracy Al^{3+} levels in soil solutions and acid mine waters. The stoichiometry of this empirical relationship, which is consistent with the solubility of jurbanite, appears to be independent of the non-carbonate mineralogical composition or texture of the spoil, soil, or geologic strata in the watershed.

Figure 4 depicts a solubility diagram similar to that used by Van Breemen (1973) and Nordstrom (1982) to demonstrate potential Al^{3+} control by aluminosilicate and basic aluminum sulfate minerals in acid sulfate waters. Soil solution and surface water composition points of the contaminated samples congregate rather well about the jurbanite solubility line at low $2pH + pSO_4$ values, whereas at values > 11, representing the uncontaminated samples, there is a tendency for undersaturation with respect to jurbanite and confinement to the region bounded by the gibbsite and kaolinite saturation lines. Only four of the 22 contaminated soil/spoil samples and about half of the surface waters were slightly undersaturated with jurbanite. These undersaturated solutions and waters, nevertheless, were still confined to the region bounded by the jurbanite and alunite solubility lines. The data suggest that precipitation of jurbanite dictates the upper limit of dissolved Al^{3+} in most soil solutions and some surface waters of contaminated areas in the watershed while alunite provides a lower solubility limit. The absence of jurbanite in the mineralogical composition of the samples studied supports Van Breemen's (1973) speculation that this mineral may be amorphous or present in quantities not detectable by XRD. Regardless of its presence or crystallinity jurbanite is only an intermediate metastable phase controlling Al^{3+} in solution, with an eventual control transfer to the more stable minerals of the system, alunite and kaolinite. Equilibrium with alunite, however, may rarely be reached because of slow nucleation and precipitation kinetics (Nordstrom, 1982). Kaolinite appears to be the most stable mineral controlling Al^{3+} in uncontaminated samples (Fig. 4). Gibbsite, K-aluminite, and basaluminite do not appear to influence dissolved Al^{3+}. These interpretations are supported by comparisons of solution ion activity products and solubility product constants of the above minerals (Tables 9, 10 and 11).

Control of Fe^{3+} in Solution

Equilibrium evaluations similar to Al^{3+} were made for soluble Fe^{3+} using amorphous $Fe(OH)_3$ (pK = -3.54), goethite (FeOOH; pK = 0.02), and jarosite $(KFe_3(SO_4)_2(OH)_6$; pK = 12.5) as potential mineral phases controlling the activity of Fe^{3+} in solution. Figure 5 depicts the relationship between pH and the negative logarithm of Fe^{3+} activity in the studied solutions and surface waters in reference to the solubility of the above minerals. The

considerable scatter of the points in the diagram suggests that the solutions do not appear to be in equilibrium with a specific Fe mineral. Although all solutions are supersaturated with goethite, their Fe^{3+} activities are considerably higher than those supported by the solubility of this mineral. Surprisingly, some of the most supersaturated solutions were those of surface waters which along with a few soil solutions supported the metastability of amorphous $Fe(OH)_3$ at low pH levels (2.75 to 4.00). The remaining contaminated solutions were mostly confined in the metastability region bound by the amorphous $Fe(OH)_3$ and the jarosite saturation lines.

A plot of the solution points, in a pH + pSO_4 versus pFe^{3+} system (Fig. 6), suggests that acid mine drainage solutions in the OH1 and OH2 watersheds obey a different regression relationship than those of BD and CL watersheds. Although the two regression lines are almost parallel to each other (slope – 1.6) the same level of pH + pSO_4 predicts higher Fe^{3+} activities in the BD and CL than in the OH watersheds. The above relationships which also imply conservative behavior are attributed to dilution effects and possible redox potential variations in the studied watersheds.

CONCLUSIONS

Dissolved Al released in ground and surface waters of acid mine drainage contaminated watersheds with low buffering capacity appeared to be controlled by the solubility of the basic aluminum sulfate minerals jurbanite and alunite. The detection of only alunite by XRD suggests that jurbanite may be amorphous or present in very small quantities. The control of soluble Al by basic aluminum sulfate minerals did not appear to be affected by the diverse mineralogical and textural compositions of the soil and geologic strata in the watershed, which may have been limited by the buffering of the pH of the systems. Soil solutions in contact with uncontaminated soil and geologic strata in the watersheds supported soluble Al levels consistent with the solubility of kaolinite. The data indicate that in solutions with pH < 4 the pH plus activity of SO_4^{2-} can accurately predict the levels of soluble Al^{3+} in surface and ground waters of the watersheds. Similar predictions can be made for soluble Fe^{3+} levels but the pH - SO_4^{2-} - Fe^{3+} relationship appears to be watershed specific.

REFERENCES

Adams, Fred. 1971. Ionic concentrations and activities in soil solutions. Soil Sci. Soc. Am. Proc. 35:420-426.

Adams, Fred, and B.F. Hajek. 1978. Effects of solution sulfate hydroxide and potassium concentrations on the crystallization of alunite, basaluminite, and gibbsite from dilute aluminum solutions. Soil Sci. 126:169-173.

American Public Health Association. 1976. Standard methods for the examination of water and wastewater. 13th ed. U.S. Government Printing Office, Washington, D.C.

Anthony, J.W., and W.J. McLean. 1976. Jurbanite, a new post-mine aluminum sulfate mineral from San Manuel Arizona. Am. Miner. 61:1-4.

Baker, J.P., and C.L. Schofield. 1982. Aluminum toxicity to fish in acidic waters. Water Air Soil Pollut., 18:289-309.

Biesecker, J.S., and J.R. George. 1966. Stress quality in Appalachia as related in coal mine drainage. 1965. Geol. Surv. Cir. 526, U.S. Geol. Surv., Washington, D.C.

Caruccio, F.T., and G. Geidel. 1978. Geochemical factors affecting coal mine drainage quality. In F.W. Schaller and P.Sutton (ed.) Reclamation of drastically Disturbed Lands. Amer. Soc. Agron., Madison, WI.

Driscoll, C.T., J.P. Baker, J.J. Bisogni, and C.L. Schofield. 1984. Aluminum speciation and equilibria in dilute acidic surface waters of the Adirondalk region of New York State. In O.R. Bricker (ed.), Acid Precipitation: Geological Aspects, Ann Arbor Sci., Ann Arbor, MI, pp. 55-75.

Evangelou, V.P., and A.D. Karathanasis. 1984. Reactions and mechanisms controlling water quality in surface-mined spoils. pp. 213-247. Symposium on the reclamation of lands disturbed by surface mining. Am. Soc. Surf. Min. Recl., Owensboro, Kentucky. July 10-13, 1984.

Frink, C.R. 1973. Aluminum chemistry in acid sulfate soils. In. H. Dost (ed.) Acid Sulfate Soils. Intern. Inst. for Land Reclamations and Improvement. Wageningen, Netherlands.

Helgeson, H.C., Garrels, R.M. and Mackenzie, F.T. 1969. Evaluation of irreversible reactions in geochemical processes involving minerals and aqueous solutions. II. Applications, Geochim. Cosmochim. Acta, 33, p. 455-481.

Johnson, N.M., C.T. Driscoll, J.S. Falon, G.E. Likens, and W.H. McDowell. 1981. Acid rain, dissolved aluminum and chemical weathering at the Hubbard Brook Experimental Forest, New Hampshire. Geochim, Cosmochim. Acta. 45:1421-1437.

Karathanasis, A.D., and B.F. Hajek. 1982. Revised methods for rapid quantitative determination of minerals in soil clays. Soil Sci. Soc. Am. J. 46:419-425.

Lindsay, W.L. 1979. Chemical equilibria in soils. John Wiley & Sons, Inc., New York.

May, H.M., P.A. Helmke, and M.L. Jackson. 1979. Gibbsite solubility and thermodynamic properties of hydroxy-aluminum ions in aqueous solution at 25°C. Geochim. Cosmochim. Acta. 43:861-868.

Nordstrom, D.K. 1982. The effect of sulfate on aluminum concentrations in natural waters: Some stability relations in the system Al_2O_3-SO_4-H_2O at 298°K. Geochim, Cosmochim. Acta. 46:681-692.

Nordstrom, D.K., and J.W. Ball. 1986. The geochemical behavior of aluminum in acidified surface waters. Sci. 232:54-56.

Nordstrom, D.K., E.A. Jenne, and J.W. Ball. 1979. Redox equilbria of iron in acid mine waters: In E.A. Jenne (ed.) Chemical Modeling in Aqueous Systems, Speciation, Sorption, Solubility and Kinetics. Am. Chem. Soc. Symp. Ser. 93, p. 51-79.

Rodriguez-Clemente, R., and Hidalgo-Lopez, A. 1985. Physical conditions in alunite precipitation as a secondary mineral. In J. I. Drever (ed.) The chemistry of weathering, p. 121-141, Reidel Publishing Company.

Rogowski, A.S., H.B. Plonke, and J.G. Broyan. 1977. Modeling the impact of strip mining and reclamation processes on quality and quantity of water in mined areas: A review. J. Env. Qual. 6:237-244.

Singh, S.S., and J.E. Brydon. 1969. Solubility of basic aluminum
sulfates at equilibrium in solution and in the presence of
montmorillonite. Soil Sci. 107-12-17.

Soil Conservation Service, USDA. 1982. Procedures for collecting soil
samples and methods of analysis for soil survey. Soil Survey
Investigations Report No. 1., U.S. Government Printing Office,
Washington, D.C.

Soil Science Society of America. 1982. Acid sulfate weathering.
SSSA. Special Publication No. 10. Madison, WI.

Stumm, W., and J.J. Morgan. 1981. Aquatic Chemistry: An introduction
emphasizing chemical equilibria in natural waters. John Wiley &
Sons, N.Y.

Van Breemen, N. 1973. Dissolved aluminum in acid sulfate soils and in
acid mine waters. Soil Sci. Soc. Am. Proc. 27:694-697.

Van Breemen, N., and K. Harmsen. 1975. Translocation of iron in acid
sulfate soils: I. Soil morphology, and the chemistry and
mineralogy of iron in a chronosequence of acid sulfate soils.
Soil Sci. Soc. Am. Proc. 39:1140-1148.

TABLE LEGEND

Table 1. Watershed characteristics.

Table 2. Sample descriptions.

Table 3. Equilibrium relationships used in this study.

Table 4. Physical and chemical properties of soil, spoil and sediment samples.

Table 5. Mineralogical composition of soil, spoil and sediment samples (< 2 mm).

Table 6. Mineralogical composition of the clay fraction (< 2 μm) of soil, spoil and sediment samples.

Table 7. Total elemental concentrations of interstitial solutions of soil, spoil and sediment samples.

Table 7a. Negative logarithms of ion activities in interstitial solutions of soil, spoil and sediment samples.

Table 8. Total elemental concentration of surface water samples.

Table 8a. Negative logarithms of ion activites in surface water samples.

Table 9. Means and standard deviations (SD) of ion activity products (pQ) for potential aluminosilicate and basic aluminum and iron sulfate minerals controlling Al^{3+} and Fe^{3+} in solution.

Table 10. Ion activity products (pQ's) for common sulfate and aluminosilicate minerals in soil solutions.

Table 11. Ion activity products (pQ's) for common sulfate and
aluminosilicate minererals in water samples.

Table 1. Watershed Characteristics.

Watershed	Location	Prevalent Rock Types	Prevalent Soil Types	Area ha	Approx. Mining Date	% Disturbed
OH1	Tributary to Muddy Creek, near Horton, Ohio County	Sandstone, siltstone and shale, Lower and Middle Pennsylvanian, Tradewater and Caseyville Formations, Mining City and Elm Lick coal beds.	Bethesda (loamy-skeletal, mixed, acid, mesic Typic Udorthents); Fairpoint (loamy-skeletal, mixed, nonacid, mesic Typic Udorthents); Zanesville (fine-silty, mixed, mesic Typic Fragiudalfs).	80	1970	70
OH2	Tributary to Bens Lick Creek, near McHenry, Ohio County			50	1970	60
BD	Tributary to Fourmile Creek near Garner, Boyd County	Sandstone interbedded with shale, Middle Pennsylvanian, Breathit Formation, Princess No. 7 coal bed.	Latham (clayey, mixed, mesic Aquic Hapludults); Shelocta (fine-loamy, mixed, mesic Typic Hapludults).	45	1960	18
CL	Tributary to an unnamed depression near Nora, Clinton County	Sandstone interbedded with shale, Middle and Lower Pennsylvanian, Breathit Formation underlain by Mississippian limestone, unnamed coal bed.	Shelocta (fine-loamy, mixed, mesic Typic Hapludults).	53	1973	16

18

Table 2. Sample description.

Watershed	Sample #	Type of Sample	Characteristics
OH1	OH-1A	spoil	Upper 10 cm of graded spoil-soil overburden material
	OH-1B	sediment	
	OH-1C	sediment	Clayey and shaly undistrubed beds below the mined coal seam percolated by acid
	OH-1D	sediment	mine drainage
	OH-1E	sediment	
	OH-1	water	Ground water seeping from spoil material
	OH-2	water	Surface stream water draining the watershed
OH2	OH-2A	spoil	Spoil material in seasonal contact with sedimentation pond-water
	OH-2B	sediment	Orange mineral precipitates on pond bank
	OH-2C	sediment	White mineral precipitates on pond bank
	OH-2D	soil	Undisturbed soil material in seasonal contact with sedimentation
	OH-2E	soil	pond water (OH-2D=A + upper B horizon, OH-2E = lower B + C horizon)
	OH-4A	spoil	Spoil bank in in seasonal contact with sedimentation pond-water
	OH-4B	spoil	Mid-slope of spoil bank
	OH-4C	spoil	Crest of spoil bank
	OH-4D	spoil	Summit of spoil bank
	OH-5A	spoil	Exposed floor of old sedimentation pond
	OH-3	water	Sedimentation pond water
	OH-4	water	Sedimentation pond water
	OH-5	water	Depression in an old sedimentation pond floor
	OH-6	water	Sedimentation pond water
BD	BD-1A	sediment	Undisturbed shaly sandstone beds over the mined coal seam
	BD-1B	soil	Depressional area and receiving acid mine drainage waters from adjacent spoil
	BD-1C	soil	bank (BD-1B = upper slope; BD-1C = lower slope)
	BD-2A	soil†	Uncontaminated sandstone bed, parent material of Shelocta soil (C horizon)
	BD-2B	soil†	Uncontaminated A and BA horizon of Shelocta soil
	BD-2C	soil†	Uncontaminated Bt horizon of Shelocta soil
	BD-3A	spoil	Highly oxidized spoil bank
	BD-3B	spoil	Spoil materials less oxidized than BD-3A
	BD-3C	soil	Subsoil material below the graded spoil bank
	BD-7	water	Flume in stream draining the strip-mined watershed
	BD-8	water	Intermittent surface water draining into the stream (60 m above flume)
	BD-9	water	Spoil seep draining into the stream (100 m above flume)
CL	CL-1A	soil†	Top soil (A + BA horizons) along stream bank (base of watershed, near flume)
	CL-1B	soil†	Subsoil (Bt + BC horizons) along stream bank (base of watershed, near flume)
	CL-2A	soil†	Surface soil (A horizon) of noncontaminated Shelocta soil
	CL-2B	soil†	Subsoil (Bt horizon) of noncontaminated Shelocta soil
	CL-2C	sediment†	Sandstone-shale interbedded C horizon of uncontaminated Shelocta soil
	CL-2D	sediment	Shaly undisturbed layer above the seam seeping acid mine drainage
	CL-10	water	Flume in stream draining the strip-mined watershed
	CL-11	water	Small pool at base of highwall.

† Uncontaminated soil and sediment samples.

19

Table 3. Equilibrium relationships used in this study.

Equation	Equilibrium Constant	Reference
$Al^{3+} + H_2O = Al(OH)^{2+} + H^+$	pK = 4.99	Adams, 1971
$Al^{3+} + 2H_2O = Al(OH)_2^+ + 2H^+$	pK = 10.13	May et al., 1979
$Al^{3+} + 3H_2O = Al(OH)_3^0 + 3H^+$	pK = 15.2	Adams, 1971
$Al^{3+} + SO_4^{2-} = AlSO_4^+$	pK = 3.2	Adams, 1971
$Fe^{3+} + H_2O = Fe(OH)^{2+} + H^+$	pK = 2.19	Lindsay, 1979
$Fe^{3+} + 2H_2O = Fe(OH)_2^+ + 2H^+$	pK = 5.69	Lindsay, 1979
$Fe^{3+} + 3H_2O = Fe(OH)_3^0 + 3H^+$	pK = 13.09	Lindsay, 1979
$Fe^{3+} + SO_4^{2} = FeSO_4^+$	pK = 4.15	Lindsay, 1979
$Al(OH)_3 = Al^{3+} + 3OH^-$ microcrystalline gibbsite	pK_{sp} = 32.65	Johnson et al., 1981
$Al(OH)_3 = Al^{3+} + 3OH^-$ well crystalline gibbsite	pK_{sp} = 33.9	Johnson et al., 1981
$KAl_3(SO_4)_2(OH)_6 = K^+ + 3Al^{3+} + 2SO_4^{2-} + 6OH^-$ alunite	pK_{sp} = 85.4	Nordstrom, 1982
$Al(SO_4)(OH)_6 + H^+ = Al^{3+} + SO_4^{2-} + H_2O$ jurbanite	pK_{sp} = 3.8	Nordstrom, 1982
$Al_4(SO_4)(OH)_{10} = 4Al^{3+} + SO_4^{2-} + 10OH^-$ basaluminite	pK_{sp} = 117.6	Nordstrom, 1982
$Al_2Si_2O_5(OH)_4 + 5H_2O = 2Al^{3+} + 2H_4SiO_4 + 6OH^-$ kaolinite	pK_{sp} = 76.4	Helgeson et al., 1969
$Fe(OH)_3 + 3H^+ = Fe^{3+} + 3H_2O$ amorphous	pK_{sp} = -3.54	Lindsay, 1979
$KFe_3(SO_4)_2(OH)_6 + 6H^+ = K^+ + 3Fe^{3+} + 2SO_4^{2-} + 6H_2O$ jarosite	pK_{sp} = 12.5	Lindsay, 1979
$FeOOH + 3H^+ = Fe^{3+} + 2H_2O$ goethite	pK_{sp} = 0.02	Lindsay, 1979

Table 4. Physical and chemical properties of soil, spoil and sediment samples.

Sample	Particle Size			Textural Class	pH†	Extractable Bases				CEC†
	Sand	Silt	Clay			Ca	Mg	K	Na	
	------ % ------					-------- cmol(+)kg^{-1} --------				
OH-1A	54.0	31.8	14.2	sl	3.48	2.28	0.63	0.03	0.19	4.38
OH-1B	14.1	50.8	36.7	sicl	3.52	1.28	2.30	0.16	0.23	19.29
OH-1C	8.8	44.7	46.5	sic	3.44	1.62	3.12	0.19	0.22	13.19
OH-1D	73.4	10.6	16.0	sl	3.51	0.93	1.72	0.07	0.17	24.88
OH-1E	17.4	24.2	58.4	c	3.35	2.32	5.43	0.24	0.28	28.27
OH-2A	41.5	38.6	19.9	l	3.50	2.63	2.60	0.10	0.58	14.04
OH-2D	27.5	52.5	20.0	sil	3.82	2.22	3.08	0.14	0.33	25.66
OH-2E	17.8	59.8	22.4	sil	3.96	1.74	3.29	0.07	0.34	8.48
OH-4A	22.8	55.1	22.1	sil	4.23	3.15	5.00	0.14	0.31	11.22
OH-4B	11.6	47.8	40.6	sic/sicl	3.77	1.64	2.22	0.19	0.22	14.70
OH-4C	12.5	44.2	43.3	sic	3.64	4.17	0.63	0.12	0.20	16.15
OH-4D	9.8	51.8	38.4	sicl	3.21	7.89	2.92	0.07	0.31	17.62
OH 5A	7.4	13.8	18.8	sil	3.20	3.76	3.71	0.07	0.20	12.05
BD-1A	21.2	54.9	23.9	sil	4.27	0.72	0.98	0.24	0.23	9.50
BD-1B	28.4	41.0	30.6	cl	3.80	0.77	0.83	0.11	0.27	12.32
BD-1C	35.5	39.4	25.1	l	3.87	0.76	0.78	0.10	0.23	13.38
BD-2A‡	84.4	11.2	4.4	ls	4.68	0.29	0.10	0.01	0.35	1.14
BD-2B‡	62.4	24.0	13.6	sl	4.37	0.34	0.18	0.05	0.34	4.71
BD-2C‡	34.1	39.6	26.3	l/cl	4.46	0.56	0.83	0.11	0.23	7.92
BD-3A	55.2	32.5	12.3	sl	3.99	0.57	0.93	0.47	0.38	6.33
BD-3B	44.3	29.7	26.0	l/cl	4.16	0.79	0.43	0.11	0.19	16.59
BD-3C	48.0	28.8	23.2	l/scl	4.03	0.58	0.22	0.08	0.18	10.30
CL-1A‡	36.2	54.6	9.2	sil	5.82	4.43	0.63	0.09	0.50	4.20
CL-1B‡	28.2	46.8	25.0	l	6.06	4.72	0.29	0.11	0.30	8.70
CL-2A‡	55.9	25.8	18.3	sl	4.73	3.67	0.79	0.18	0.20	12.00
CL-2B‡	39.6	29.0	31.4	cl	4.61	0.74	0.29	0.15	0.19	11.22
CL-2C‡	28.6	34.3	37.1	cl	4.44	0.61	0.41	0.15	0.20	14.36
CL-2D	63.2	25.9	10.9	sl	4.06	0.81	1.18	0.09	0.18	6.55

† pH = 1:1 soil: water; CEC = NH$_4$OAC pH 7
‡ Uncontaminated samples

Table 5. Mineralogical composition[†] of soil, spoil and sediment samples (< 2 mm).

Sample	V/HIV	INT	MI	K	Q	GO	F	GY	AM	BA	HBA	JAR	AL
							$g\ kg^{-1} \times 10^{-1}$						
OH-1A	—	—	17	12	36	—	23	—	—	—	—	5	—
OH-1B	6	3	10	12	55	—	9	—	—	—	—	5	7
OH-1C	—	—	20	16	45	6	8	—	—	—	—	3	—
OH-1D	—	—	10	15	29	16	9	—	2	—	—	10	8
OH-1E	6	6	12	15	24	8	10	—	3	—	—	9	7
OH-2A	5	5	12	10	24	4	11	—	3	—	—	18	9
OH-2B[‡]	—	—	—	—	—	—	—	—	—	—	—	—	—
OH-2C[‡]	—	—	—	—	—	—	—	—	—	—	—	—	—
OH-2D	4	—	7	7	62	—	9	6	2	6	—	—	5
OH-2E	3	—	5	6	67	—	9	—	3	2	—	—	—
OH-4A	7	—	18	14	43	—	15	—	2	—	—	—	—
OH-4B	3	—	11	9	21	—	49	10	—	—	—	5	—
OH-4C	6	—	16	14	27	—	10	4	—	—	—	17	—
OH-4D	4	—	9	9	22	—	3	—	—	3	—	38	8
OH 5A	—	—	9	20	43	—	9	—	3	3	—	5	8
BD-1A	6	—	25	13	28	4	5	10	5	4	—	4	10
BD-1B	6	—	11	15	34	—	9	9	—	5	4	4	3
BD-1C	6	—	13	17	32	3	8	—	—	—	—	4	3
BD-2A§	3	—	10	29	35	—	23	—	—	—	—	—	—
BD-2B§	4	—	13	20	50	3	10	—	—	—	—	—	—
BD-2C§	5	—	19	13	51	3	9	—	—	—	—	—	—
BD-3A	—	—	19	3	47	—	8	10	4	2	—	3	4
BD-3B	10	—	13	15	41	—	7	8	2	2	—	2	—
BD-3C	8	—	10	18	43	—	9	6	2	2	—	—	2
CL-1A§	—	—	5	3	79	—	8	—	—	—	—	—	5
CL-1B§	—	—	3	2	82	—	5	—	3	—	2	—	3
CL-2A§	—	—	11	11	66	—	4	—	2	2	—	2	2
CL-2B§	—	—	19	14	53	—	7	—	3	3	—	4	—
CL-2C§	—	—	12	18	47	—	7	4	—	—	4	4	—
CL-2D	—	—	14	13	52	—	9	—	3	—	—	6	3

[†] AL = Alunite; AM = Aluminite; BA = Basaluminite; F = Feldspars;
GI = Gibbsite; GO = Goethite; GY = Gypsum; HBA = Hydrobasaluminite; HIV = Hydroxyinterlayered Vermiculite; INT = Interstratified; JAR = Jarosite; K = Kaolinite; MI = Mica; Q = Quartz; SM = Smectite; V = Vermiculite.
[‡] amorphous precipitates
§ Uncontaminated samples

Table 6. Mineralogical compositon[†] of the clay fraction (<2 mm) of soil, spoil and sediment samples.

Sample	SM	V	HIV	INT	MI	K	Q	GO	F	AM	BA	JAR	AL	GI
						g kg^{-1} X 10^{-1}								
OH-1A	--	8	--	8	12	34	3	5	5	--	--	15	20	--
OH-1B	14	12	--	4	14	24	16	5	5	--	--	6	--	--
OH-1C	--	--	--	11	23	48	8	5	--	5	--	--	--	--
OH-1D	17	12	--	--	18	31	3	4	3	--	--	12	--	--
OH-1E	23	--	--	15	11	27	7	7	3	--	--	7	--	--
OH-2A	--	8	--	8	13	27	5	4	4	--	--	31	--	--
OH-2B‡	--	--	--	--	--	--	--	--	--	--	--	--	--	--
OH-2C‡	--	--	--	--	--	--	--	--	--	--	--	--	--	--
OH-2D	--	--	13	6	11	60	5	5	--	--	--	--	--	--
OH-2E	--	--	17	10	12	45	6	4	2	--	--	--	--	4
OH-4A	--	--	7	6	17	52	6	4	5	--	4	4	--	--
OH-4B	--	10	--	10	15	34	5	4	7	--	--	17	--	--
OH-4C	--	--	6	--	10	20	9	--	4	--	4	44	--	--
OH-4D	--	--	10	--	10	18	10	8	--	--	--	40	--	--
OH-5A	--	--	11	18	18	40	5	--	--	--	--	7	--	--
BD-1A	--	7	--	--	21	55	5	4	4	--	--	4	--	--
BD-1B	--	11	--	10	21	46	5	4	3	--	--	--	--	--
BD-1C‡	--	--	10	10	22	51	7	--	--	--	--	--	--	--
BD-2A‡	--	--	7	--	21	66	3	--	3	--	--	--	--	--
BD-2B‡	--	--	12	5	14	61	6	--	2	--	--	--	--	--
BD-2C‡	--	--	12	11	13	54	3	4	3	--	--	--	--	--
BD-3A	--	--	--	15	50	20	10	--	5	--	--	--	--	--
BD-3B	--	--	12	5	15	47	8	4	2	3	2	2	--	--
BD-3C	--	--	15	8	13	55	3	3	1	--	--	2	--	--
CL-1A‡	--	--	30	--	8	40	12	4	--	--	--	--	--	6
CL-1B‡	--	--	47	--	7	36	10	--	--	--	--	--	--	--
CL-2A‡	--	10	--	10	18	44	4	4	4	4	--	--	--	--
CL-2B‡	3	--	9	14	14	55	4	--	--	--	--	--	--	--
CL-2C‡	--	10	--	14	17	51	5	3	--	--	--	--	--	--
CL-2D	--	8	--	9	16	30	--	--	--	--	--	12	25	--

† See Table 4 for mineral symbols.
‡ Uncontaminated samples

23

Table 7. Total elemental concentrations of interstitial solutions of soil, spoil and sediment samples.

Sample	pH	Al	Fe§	Na	K	Ca	Mg	Mn	Si	SO$_4$	Cl
						----mM----					
OH-1A	2.78	2.66	0.13 (0.04)	0.37	0.02	11.06	2.92	0.27	3.39	18.12	0.03
OH-1B	3.20	10.33	0.05 (0)	2.20	0.21	4.61	11.54	1.53	3.16	32.56	0.23
OH-1C	2.56	8.52	0.64 (0.49)	1.13	0.20	8.01	18.58	2.18	0.83	39.68	0.17
OH-1D	2.63	5.00	0.14 (0.05)	0.76	0.03	4.88	10.71	2.74	1.57	23.34	0.01
OH-1E	2.71	4.93	3.47 (0.15)	0.81	0.01	5.47	13.00	3.20	2.16	25.93	0.27
OH-2A	3.61	1.93	0.37x10^{-2} (0)	0.96	0.09	6.00	8.50	0.81	1.57	16.87	1.51
OH-2D	3.96	0.74	0.16x10^{-2} (0)	1.46	0.67	8.54	7.79	5.37	1.05	18.21	0.32
OH-2E	3.61	1.88	1.15 (0.76)	3.12	0.50	10.66	18.83	3.92	0.77	33.75	0.24
OH-4A	3.82	0.35	0.17x10^{-2} (0)	0.93	0.58	10.01	16.42	6.39	1.25	27.50	0.02
OH-4B	3.87	0.14	0.07x10^{-2} (0)	0.21	0.24	0.53	0.46	0.03	0.43	1.44	0.00
OH-4C	3.86	0.51	0.07x10^{-2} (0)	0.67	0.22	7.50	1.15	0.02	0.72	9.53	0.12
OH-4D	2.73	30.30	1.66 (0.14)	0.24	0.03	10.43	17.87	15.66	3.07	73.59	0.10
OH-5A	1.96	195.93	410.03 (15.7)	0.04	0.05x10^{-1}	10.10	162.08	9.38	ND†	ND	ND
BD-1A	3.86	0.14	0.28x10^{-2} (0)	2.45	0.43	0.33	0.38	0.04	0.50	1.12	2.24
BD-1B	3.50	0.64	0.04 (0)	0.53	0.13	1.10	1.57	0.18	0.43	3.75	0.34
BD-1C	3.43	0.94	0.18 (0)	0.62	0.13	1.45	1.97	0.34	1.10	5.15	0.06
BD-2A‡	4.40	0.05x10^{-1}	0.01x10^{-2} (0)	0.07	0.13	0.06	0.06	0.07x10^{-1}	0.30	0.25	0.00
BD-2B‡	4.33	0.02x10^{-1}	0.07x10^{-2} (0)	0.55	ND	0.17	ND	ND	0.21	ND	ND
BD-2C‡	4.35	ND†	0.37x10^{-2} (0)	0.35	ND	0.12	ND	ND	0.27	ND	ND
BD-3A	3.26	2.59	0.20x10^{-2} (0)	5.34	1.63	3.41	6.70	0.10	2.79	17.34	0.10
BD-3B	3.86	0.01	0.17x10^{-2} (0)	0.07	0.12	0.27	0.17	0.05	0.11	0.50	0.09
BD-3C	3.97	0.06	0.07x10^{-2} (0)	0.08	0.08	0.30	0.14	0.07	1.16	0.62	0.00
CL-1A‡	5.71	0.01x10^{-1}	0.07x10^{-2} (0)	0.28	0.07	0.57	0.51	0.07x10^{-2}	0.15	0.30	1.74
CL-1B‡	5.51	0.02x10^{-2}	0.12x10^{-2} (0)	0.04	0.06x10^{-1}	0.11	0.01	0.00	0.13	0.06	0.16
CL-2A‡	4.78	0.05	0.00	0.35	0.86	0.90	1.65	0.05	0.32	0.69	4.57
CL-2B‡	4.52	0.07x10^{-1}	0.03x10^{-2} (0)	0.06	0.08x10^{-1}	0.06	0.02	0.05x10^{-1}	0.16	0.16	0.00
CL-2C‡	4.32	0.01	0.12x10^{-2} (0)	0.08	0.10	0.09	0.07x10^{-1}	0.07x10^{-1}	0.18	0.27	0.28
CL-2D	3.24	3.66	0.23 (0)	0.72	0.08	3.75	8.83	0.46	2.96	18.34	0.05

† ND = not determined due to insufficient amount of solution.
‡ Uncontaminated samples
§ Values in parenthesis represent Fe^{2+} concentrations measured by the orthophenan thraline method (ALPHA, 1976).

Table 7a. Negative logarithms of ion activities in interstitial soil solutions.

Sample	pH	pNa$^+$	pK$^+$	pCa^{2+}	pMg^{2+}	pMn^{2+}	pSO$_4^{2-}$	pCl$^-$	pAl^{3+}	pFe^{3+}
OH-1A	2.78	3.55	4.72	2.45	3.00	4.05	2.22	4.52	3.70	5.88
OH-1B	3.20	2.79	3.84	2.95	2.52	3.43	2.01	3.64	3.29	6.52
OH-1C	2.56	3.09	3.89	2.73	2.32	3.29	2.00	3.77	3.39	5.36
OH-1D	2.63	3.24	4.66	2.85	2.48	3.10	2.15	5.15	3.49	5.87
OH-1E	2.71	3.21	5.09	6.48	2.40	3.05	2.14	3.57	3.52	4.49
OH-2A	3.61	3.12	4.15	2.71	2.52	3.58	2.27	2.82	3.82	7.57
OH-2D	3.96	2.95	3.28	2.56	2.57	3.37	2.26	3.50	4.25	8.28
OH-2E	3.61	2.64	3.44	2.56	2.27	3.24	2.10	3.62	3.98	5.18
OH-4A	3.82	3.16	3.36	2.56	2.31	3.74	2.15	4.70	4.66	8.15
OH-4B	3.52	3.70	3.66	3.46	3.51	4.70	3.01	0	4.40	8.40
OH-4C	3.33	3.57	4.19	2.52	3.32	5.01	2.42	3.92	4.26	8.49
OH-4D	2.73	3.82	4.77	2.77	2.49	4.20	1.75	4.02	3.06	5.91
OH-5A										
BD-1A	3.86	2.65	3.41	3.66	3.58	4.52	3.13	2.65	4.39	7.77
BD-1B	3.50	3.33	3.94	3.24	3.07	4.00	2.69	3.47	3.96	6.26
BD-1C	3.43	3.27	3.94	3.15	3.01	3.80	2.58	4.22	3.85	5.59
BD-2A	4.40	4.15	3.90	4.30	4.15	5.22	3.67	0	5.77	10.16
BD-2B										
BD-2C										
BD-3A	3.26	2.38	2.90	2.97	2.64	4.52	2.21	4.00	3.74	7.67
BD-3B	3.86	4.15	3.93	3.68	3.89	4.40	3.41	4.04	5.32	7.98
BD-3C	3.97	4.10	4.12	3.64	4.00	4.30	3.32	0	4.64	8.54
CL-1A	5.71	3.72	4.19	3.37	3.11	6.30	3.69	2.76	8.68	11.90
CL-1B	5.51	4.40	5.22	4.00	5.40	0	4.25	3.79	8.03	11.26
CL-2A	4.78	3.49	3.11	3.23	2.96	4.40	3.42	2.34	5.36	9.91
CL-2B	4.52	4.22	4.11	4.30	4.70	5.37	3.84	0	5.74	8.93
CL-2C	4.32	3.42	4.04	4.10	4.30	5.22	3.65	3.55	5.46	5.67
CL-2D	3.24	3.25	4.21	2.93	2.53	3.85	2.20	4.30	3.58	

Table 8. Total elemental concentrations of surface water samples.

Sample	pH	Al	Fe†	Na	Mg	Ca	K	Si	SO$_4$	Cl
						--mM--				
OH-1	2.81	4.29	1.21 (0.09)	1.13	16.27	6.66	0.19	1.16	4.25	39.81
OH-2	3.08	0.64	1.05 (0.04)	1.05	7.21	3.51	0.28	0.54	12.25	0.02
OH-3	3.25	0.86	0.90 (0.02)	0.90	9.33	5.70	0.12	0.76	16.72	0.00
OH-4	2.80	1.94	1.02 (0.04)	1.02	1.84	10.40	0.40	1.18	32.06	0.24
OH-5	2.72	26.00	3.59 (0.39)	3.59	84.58	11.28	0.08×10^{-1}	0.15	135.47	0.21
OH-6	3.36	0.18	0.42 (0)	0.42	7.10	6.0	0.26	0.44	13.62	0.00
BD-7	3.30	0.23	0.93 (0)	0.93	0.68	0.83	0.13	0.55	2.34	0.05
BD-8	3.72	0.66	1.92 (0)	1.92	1.59	1.31	0.11	0.74	4.84	0.10
BD-9	4.03	0.71	2.06 (0)	2.06	1.36	1.23	0.09	0.65	4.65	0.13
CL-10	6.30	0.00	0.20 (0)	0.20	0.36	0.69	0.79	0.05	1.63	0.00
CL-11	3.79	2.70	0.07 (0)	0.07	3.83	1.85	0.06	1.49	9.72	0.05

† Values in parenthesis represent Fe^{2+} concentrations measured by the orthophenananthroline method (APHA, 1976).

Table 8a. Negative logarithms of ion activities in water samples.

Sample	pH	pNa^+	pK^+	pCa^{2+}	pMg^{2+}	pMn^{2+}	pSO_4^{2-}	pCl^-	pAl^{3+}	pFe^{3+}
OH-1	2.81	3.05	3.83	2.57	2.15	0	3.00	1.40	3.18	4.24
OH-2	3.08	3.07	3.66	2.89	2.55	0	2.35	4.77	4.22	4.84
OH-3	3.25	3.15	4.02	2.73	2.48	0	2.27	5.19	4.16	5.03
OH-4	2.80	3.12	3.54	2.57	2.28	0	2.10	3.62	3.96	5.07
OH-5	2.72	2.66	5.31	2.80	1.87	0	1.70	3.68	3.19	4.90
OH-6	3.36	3.47	3.69	2.67	2.57	0	2.33	5.41	4.79	5.35
BD-7	3.30	3.08	3.92	3.31	3.39	0	2.84	4.29	4.29	4.67
BD-8	3.72	2.78	4.01	3.19	3.10	0	2.59	4.00	4.00	4.82
BD-9	4.03	2.75	4.11	3.22	3.15	0	2.60	3.90	3.98	5.17
CL-10	6.30	3.75	3.14	3.35	3.64	0	2.96	0	8.45	13.89
CL-11	3.79	4.27	4.31	3.14	2.80	0	2.36	4.30	3.58	6.40

Table 9. Means and standard deviations (SD) of ion activity products (pQ) for potential aluminosilicate and basic aluminum and iron sulfate minerals controlling Al^{3+} and Fe^{3+} in solution.

Samples		Gibbsite	Kaolinite	Alunite	Jurbanite	Basaluminite	Jarosite
Uncontaminated soil solutions	pQ[†]	33.6	74.7	85.1	5.1	120.0	13.9
	SD	±0.9	±1.7	±2.3	±0.9	±2.7	±1.2
Contaminated soil solutions	pQ[†]	34.3	77.7	84.6	3.0	124.8	9.5
	SD	±7.5	±1.9	±2.1	±0.7	±3.1	±3.1
Surface waters	pQ[†]	35.6	77.9	84.5	3.2	124.2	5.1
	SD	±1.8	±3.3	±2.6	±0.8	±5.3	±3.2
Reference minerals	pK[‡]	33.9	76.4	85.4	3.8	117.6	12.5

[†]$pQ = pAl^{3+} + 3pOH^-$ for gibbsite; $2pAl^{3+} + 2pH_4SiO_4 + 6pOH^-$ for kaolinite; $pK^+ + 3pAl^{3+} + 2pSO_4^{2-} + 6pOH^-$ for alunite; $pAl^{3+} + pSO_4^{2-} - pH$ for jurbanite; $4pAl^{3+} + pSO_4^{2-} + 10pOH^-$ for basaluminite; and $pK^+ + 3pFe^{3+} + 2pSO_4^{2-} - 6pH$ for jarosite.
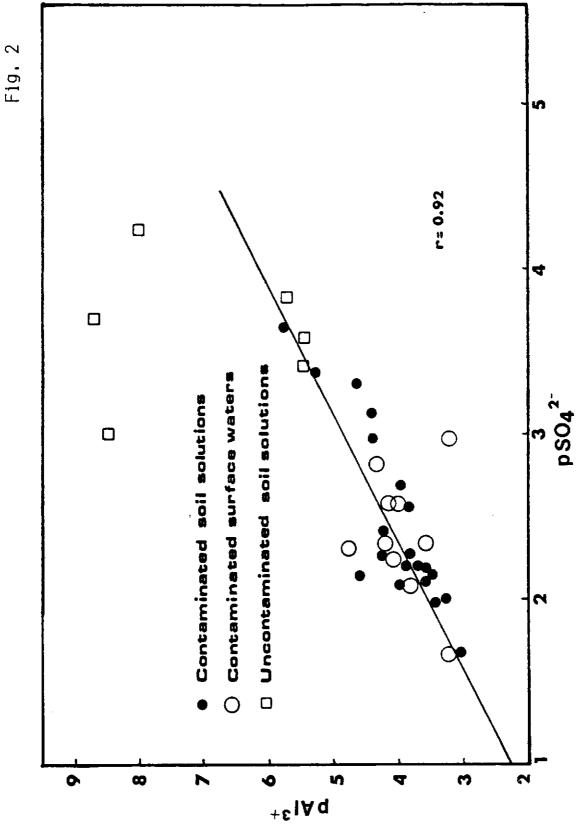
[‡] solubility product constant.

28

Table 10. Ion activity products (pQ's) for common sulfate and aluminosilicate minerals in soil solutions.

Sample	Gypsum	Gibbsite	Alunite	Kaolinite	Jarosite	Jurbanite	Basaluminite
OH-1A	4.67	37.36	87.58	79.66	10.12	3.14	129.23
OH-1B	4.96	35.69	82.53	76.39	8.22	2.10	123.18
OH-1C	4.73	37.71	86.70	81.59	8.61	2.83	129.97
OH-1D	5.00	37.60	87.65	80.81	10.79	3.01	129.81
OH-1E	4.95	37.38	87.67	80.10	6.58	2.95	129.10
OH-2A	4.97	34.98	82.49	75.58	9.74	2.48	121.43
OH-2D	4.82	34.37	80.79	74.70	8.88	2.55	119.66
OH-2E	4.65	35.14	81.92	76.53	1.52	2.47	121.91
OH-4A	4.71	35.19	82.72	76.20	9.19	2.99	122.58
OH-4B	6.46	35.83	85.76	78.30	13.76	3.89	125.40
OH-4C	4.94	36.26	85.83	78.81	14.52	3.35	126.14
OH-4D	4.52	36.87	85.07	78.76	10.91	2.08	126.68
OH-5A							
BD-1A	6.78	34.80	83.68	76.21	9.82	3.66	122.07
BD-1B	5.92	35.44	84.20	77.63	7.10	3.15	123.47
BD-1C	5.74	35.56	84.07	77.05	5.29	3.00	123.70
BD-2A	7.95	34.56	86.15	76.19	15.32	5.04	122.74
BD-2B							
BD-2C							
BD-3A	5.17	35.94	82.98	77.00	10.77	2.69	124.50
BD-3B	7.09	35.74	87.55	79.42	11.53	4.87	126.09
BD-3C	6.96	34.73	84.86	75.33	12.56	3.99	122.18
CL-1A	7.05	33.54	87.35	74.71	13.01	6.66	121.30
CL-1B	8.26	33.50	88.75	74.79	14.44	6.77	121.28
CL-2A	6.65	33.01	81.35	73.03		4.00	117.04
CL-2B	8.14	34.18	85.89	75.95	14.40	5.06	121.61
CL-2C	7.76	34.48	85.80	76.48	12.21	4.79	122.23
CL-2D	5.13	35.85	83.91	76.77	6.18	2.54	124.12
Reference pK's	4.6	33.9	85.4	76.4	12.5	3.8	117.6

Table 11. Ion activity products (pQ's) for common sulfate and aluminosilicate minerals in water samples.

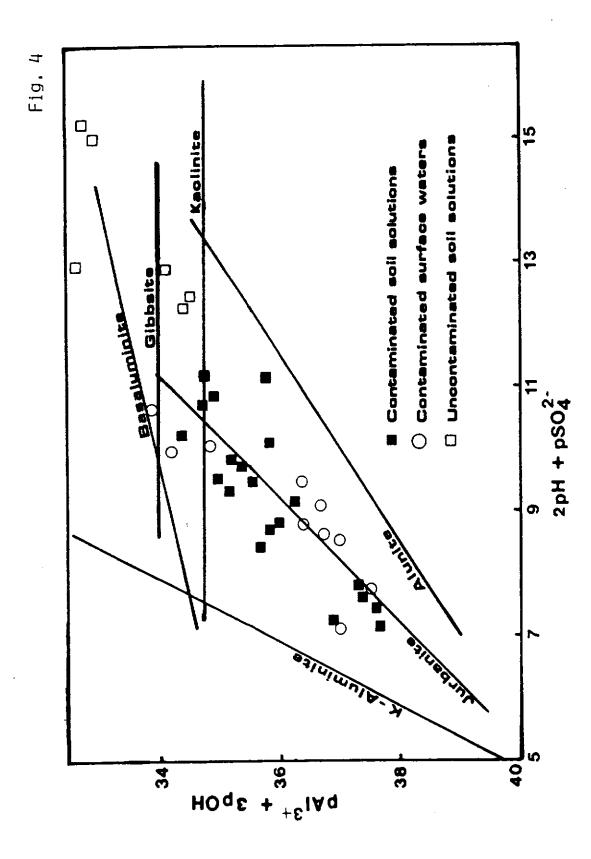| Sample	Gypsum	Gibbsite	Alunite	Kaolinite	Jarosite	Jurbanite	Basaluminite
OH-1	5.57	36.75	86.51	79.37	5.69	3.37	127.62
OH-2	5.23	36.97	86.54	80.50	4.40	3.49	128.42
OH-3	4.99	36.41	85.54	79.07	4.15	3.18	126.42
OH-4	4.66	37.56	86.82	80.98	6.15	3.26	129.93
OH-5	4.49	37.03	85.96	81.69	7.09	2.17	127.25
OH-6	5.00	36.70	86.56	80.13	4.24	3.76	127.87
BD-7	6.14	36.38	86.67	79.29	3.81	3.83	126.99
BD-8	5.78	34.84	82.87	75.95	1.33	2.87	121.40
BD-9	5.81	33.89	81.07	74.16	0.64	2.55	118.23
CL-10	6.31	31.55	80.61	71.72	12.93	5.11	113.76
CL-11	5.50	34.20	81.03	74.06	5.49	2.15	118.76
Reference pK's	4.6	33.9	85.4	76.4	12.5	3.8	117.6

FIGURE LEGEND

Fig. 1. Values of pH and pAl^{3+} for soil/spoil/sediment solutions and surface waters in reference to jurbanite, kaolinite and gibbsite solubility lines (pH_4SiO_4 = 3.5; pSO_4^{2-} = 3.0).

Fig. 2. Relationship between pAl^{3+} and pSO_4^{2-} in soil/spoil/sediment solutions and surface waters.

Fig. 3. Relationship between pAl^{3+} versus $2pH + pSO_4^{2-}$ in soil/spoil/sediment solutions and surface waters.

Fig. 4. Solubility diagram for potential aluminosilicate and basic aluminum sulfate minerals controlling dissolved Al^{3+} in the pAl^{3+} versus $2pH + pSO_4^{2-}$ system.

Fig. 5. Values of pH and pFe^{3+} for soil/spoil/sediment solutions and surface waters in reference ot goethite, amorphous $Fe(OH)_3$, and jarosite solubility lines.

Fig. 6. Relationship between pFe^{3+} and $pH + pSO_4^{2-}$ in soil/spoil/sediment solutions and surface waters of the studied watersheds.

Fig. 1

- Contaminated soil solutions
- Contaminated surface waters
- Uncontaminated soil solutions

Kaolinite Gibbsite Microcrystalline Gibbsite

Gibbsite

Surbanite

pH

pAl^{3+}

Fig. 2

r = 0.92

pSO₄²⁻ → pSO_4^{2-}

pAl³⁺ → pAl^{3+}

● Contaminated soil solutions
○ Contaminated surface waters
□ Uncontaminated soil solutions

Fig. 3

$pH + pSO_4^{2-}$

pAl^{3+}

● Contaminated soil solutions
○ Contaminated surface waters
□ Uncontaminated soil solutions

$(pAl^{3+} = 2/3(pH+pSO_4{}^{2-})+0.05; \ R^2 = 0.85)$

Fig. 4

■ Contaminated soil solutions
○ Contaminated surface waters
□ Uncontaminated soil solutions

$2pH + pSO_4^{2-}$

$pAl^{3+} + 3pOH$

Basaluminite

Gibbsite

Kaolinite

Alunite

Jurbanite

K-Aluminite

35

Fig. 5

● Contaminated soil solutions
○ Contaminated surface waters
□ Uncontaminated soil solutions

Goethite

Jarosite (pSO_4 12)

Jarosite (pSO_4 = 4)

$Fe(OH)_3$ am
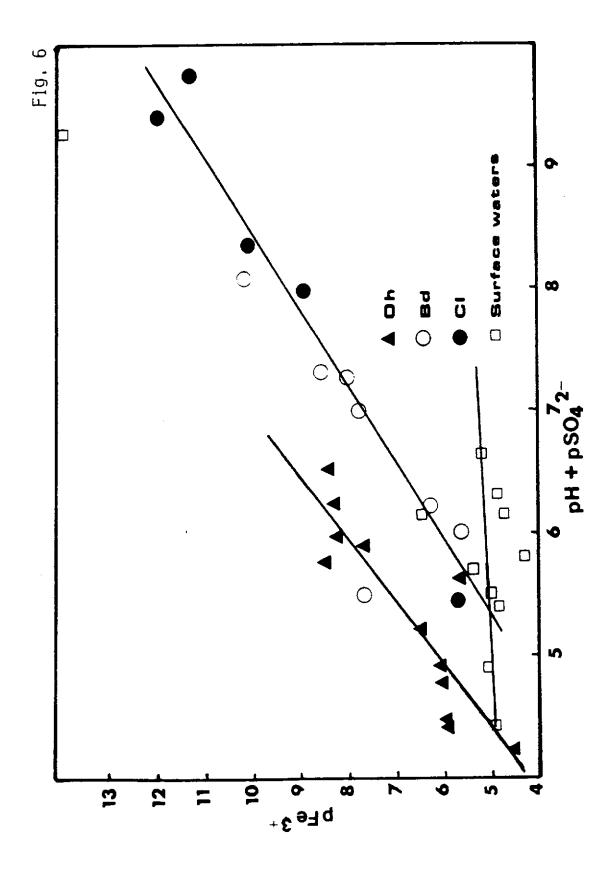
pH

pFe^{3+}

Fig. 6

PART II

KINETICS OF AL AND FE RELEASE

PART II

INTRODUCTION

When sulfate enriched acid mine drainages interact with soil and geological materials they form soluble Al and Fe sulfate compounds capable of releasing toxic levels of Al and Fe into adjacent water reservoirs (Caruccio and Geidel, 1978; Driscoll et al., 1984; Evangelou and Karathanasis, 1984; Nordstrom et al., 1979; Van Breeman, 1973; Harmsen and Van Breemen, 1975). Using equilibrium models researchers have suggested that in addition to gibbsite and kaolinite, aluminum sulfate minerals, such as jurbanite, alunite, basaluminite, and aluminite may control the solubility of Al in solutions percolating through these systems (Nordstrom 1982; Nordstrom and Ball, 1986; Anthony and McLean, 1976; Rodriguez-(Clemente and Hidalgo-Lopez, 1985; Karathanasis et al., 1988; Van Breemen, 1973; Johnson et al., 1981). Similarly, in addition to the various Fe-hydroxides (goethite, amorphorus $Fe(OH)_3$), jarosite (K $Fe_3(SO_4)_2(OH)_6$) may control the solubility of Fe^{3+} in effluents of such systems (Harmsen and Van Breemen, 1975; Nordstrom et al., 1979; Singer and Stumm, 1968; Karathanasis et al., 1988). Thermodynamic equilibrium models utilizing the solubility product principle, although useful, present several inherent limitations in accurately predicting Al and Fe behavior in acid mine drainage contaminated watersheds because they are open, heterogeneous and non-equilibrium systems. Furthermore, these models do not take into account kinetic effects that can drastically change the composition of the system over time. This is because the amount and rate of Al and Fe released from the contaminated watershed depends not only on the solubility of the mineral controlling Al and Fe in the effluent but also on physicochemical, mineralogical and hydrological factors controlling the rate of water flow through the soil or geological materials (Rogowski et al., 1977; Lewis and Grant, 1979; Singer and Stumm, 1968; Lowry and Finney, 1962; Longbein and Dowdy, 1964). Significant variations in the chemistry of stream waters draining acid mine contaminated watersheds have been observed as a function of discharge including dilution, concentration or no change by increasing discharge (Johnson et al., 1969). These chemical changes can be explained variously in terms of reaction kinetics (Longbein and Dowdy, 1964) or on the basis of simple mixing models (Johnson et al., 1969; Hall, 1970).

Experimental leaching studies of pyritic coal mine spoil materials designed to predict long term potential acidity also have suggested drastic changes both in dominant chemical species and in concentration over a long time period. In a system with moderate pyrite and low carbonate content, the evolution of drainage water chemistry may progress from an effluent with a high SO_4-moderate pH, upon exhaustion of the available carbonates, to that with a low pH-high SO_4, and then to one with a low SO_4-moderate pH upon exhaustion of the available pyrite in the oxidation zone (Vimmerstedt and Struthers, 1968). These chemical changes over time suggest that the solubility control of Al and Fe in effluents of these systems may be transferred to various minerals, following a mineral sequence pattern which is site and material specific.

The objective of this study was to determine the effect of water percolating at different flow rates through acid sulfate drainage inflicted spoil, soil, and geological materials on the amount of Al and Fe released in a given aquifer.

MATERIALS AND METHODS

Two pyritic spoil materials represented by samples OH-4D and BD-3A, two contaminated sediment samples represented by samples OH-1E and CL-2D, and two soil samples (one contaminated by acid mine drainage, BD-1C; the other almost uncontaminated, CL-1A) were selected for the leaching column experiments. The pysicochemical and mineralogical properties of these materials and of the watersheds from which they were sampled are listed in Tables 1, 2, 4, 5 and 6 of part I. Compositions of in situ solutions contacting these material are listed in Tables 7, 7a, 8 and 8a of part I.

The samples were air-dried, ground and sieved through a 2-mm sieve and packed into 50 cm long plexiglass columns of 6 cm diameter. The height of the material in the column was approximately 40 cm. The lower end of each column was attached to a funnel with a 0.45 νm pore size filter. A drainage tube was attached to the funnel draining the effluent into a collection flask. The top of each column was closed with a rubber stop with two openings. One of the openings was used as inlet for the leaching solution and the other for aeration. The inlet tubes of each column were connected to distilled water reservoirs, which provided water flow rates of 1 and 3 ml/hr to two sets of duplicated columns. The water flow rates were adjusted and regulated by a persistaltic pump. Decreasing hydraulic conductivity problems occurred in several of the columns (especially with the 3 ml/hr flow rate set) in 3 to 4 instances during the experiment. At that time the water flow was stopped in all columns to prevent overflow and restarted after 5 days to allow stabilization of particle distribution. These stabilization periods also served to study the effect of simulated alternating wetting and drying cycles on effluent compositions. Effluent samples were collected at certain time intervals and at the beginning and end of each wetting cycle over a period of 120-150 days. The effluent samples were analyzed in duplicate for pH, Al, Fe, Ca, Mg, K, Na, Mn, Si, S and Cl according to methods listed in part I of this report. Solution ionic activities were calculated by using the extended Debye-Huckel equation and a method of successive approximations (Adams, 1971), and are reported in Tables 1 through 6a. Ionic speciations were based on dissociation and solubility product constants listed in Table 3.

RESULTS AND DISCUSSION

Changes in Effluent Solution Composition with Time

Figures 1, 2, 3, 4, 5, and 6 show effluent composition changes in pH, SO_4^{2-}, Al, Ca and Mg, respectively, during the 5 months of the experiment. Some major spikes in the distribution of elements are associated with the beginning of a new wetting cycle. The smaller deviations (smaller peaks) in the distribution curves of each element are the result of fluctuations in the hydraulic conductivity of the materials during the course of the experiment.

The composition point distribution in Figure 1 indicates that while there was a very small rise in the pH of effluents BD-3A, OH-4D, CL-2D, and OH-1E during the 120 day period, sharp pH increases occurred in the effluents of CL-1A (4.8 to 8.3) and BD-1C (3.0 to 5.5) samples after 20 and 38 days of leaching, respectively. The fact that the pH of these two samples remained relatively constant for the rest of the experiment suggests that a new pH steady state was established after the specified critical time period. The only other sample showing a moderate but gradual pH increase (2.25 to 3.0) was the OH-4D effluent.

The sharp pH increase in the CL-1A and BD-3A effluents correlates quite well with the drastic decrease of SO_4^{2-} concentrations from about 14.0 to almost 0.0 mM after 20 days (CL-1A) and from about 14.0 to about 1.0 mM after 40 days (BD-3A) of leaching (Fig. 2). Apparently, after the dissolution and removal of sulfate salts another mechanism prevails and assumes control of the pH in the effluents of these samples. Although significant decreases in SO_4^{2-} concentrations also occurred in all effluents (Fig. 2), the reduction was not adequate to change the existing pH control mechanism.

The pH or SO_4^{2-} changes also had drastic effects on the Al concentration of most effluents (Fig. 3). Aluminum concentrations were 2 to 3 times lower after 120 leaching days. For most of the samples this reduction occurred between the 20 and 40 day period, except for OH-4D, which showed a gradual decrease throughout the experiment. These decreases were even more spectacular for the activity of Al^{3+}, dropping 10^8 times in effluent CL-1A, 10^4 times in BD-1C, 10^2 times in OH-4D, CL-2D, and OH-1E and about 5 times in the BD-3A effluent (Fig. 4).

The fact that the sum of Ca+Mg (mM) leached from the CL-1A and BD-1C samples is about equal to the total mM of SO_4^{2-} suggests that the complete dissolution and removal of Ca and Mg sulfate salts may be responsible for the dramatic pH, SO_4^{2-} and Al^{3+} changes in these particular samples (Fig. 5 and 6). The constant Ca concentration in the OH-4D effluent during the experiment and the presence of abundant SO_4^{2-} suggests equilibrium with gypsum (Fig. 5).

These elemental distributions were consistent in both 1 and 3 ml/hr flow rates. Greater consistency, however, was observed with the 1ml/hr rate because they posed fewer problems in terms of uniformity of hydraulic conductivity and regulation of the water flow.

Effect of Kinetics on Al Solubility Control

Effluents from the two spoil materials OH-4D and BD-3A remained saturated with respect to jurbanite during the entire length of the leaching experiment (Fig. 7). This is also illustrated from the clustering of the effluent composition points around the jurbanite solubility line in Fig. 8 and 9, indicating a near equilibrium condition of these solutions with the above mineral. The uniform distribution pattern of both 1 and 3 ml/hr effluents suggests no apparent effect of the flow rate on soluble Al levels released by these materials. It should be pointed out, however, that the majority of the BD-3A effluent points are also confined in the region bounded by the kaolinite and gibbsite solubility lines, suggesting possible control of Al in these samples also by the above minerals. In contrast, soluble Al levels in effluents of CL-1A, BD-1C, and CL-2D dropped below the jurbanite solubility limit within two weeks of leaching, while the OH-1E effluent supported Al concentrations within the range of jurbanite solubility for the first 45 days and gradually became undersaturated thereafter (Fig. 7).

It is also evident from Fig. 10 that Al levels in the CL-1A effluents after a few days of leaching, became consistent with the solubility of microcrystalline gibbsite, when the few sulfates present in the original material were completely dissolved. A similar trend is also observed in the BD-1C effluents (Fig. 11), where Al concentrations were confined in the region bounded by the jurbanite-alunite saturation lines during most of the experiment, but moving gradually towards the gibbsite and microcrystalline gibbsite solubility regions, where they concentrate during the final stages of

43

leaching. Again as was the case with the other materials there is no apparent effect of the different flow rates.

A somewhat different pattern of Al solubility control was observed in the CL-2D and OH-1E samples. Aluminum levels in effluents of both of these samples, after an original saturation with jurbanite, appeared to move away from jurbanite and eventually became consistent with the solubility of alunite (Fig. 12 and 13). The Al control transfer from jurbanite to alunite appears to occur faster in the CL-2D material and much slower in the OH-1E material. This is probably the result of the higher buffering capacity of the OH-1E (higher clay content and CEC, presence of expanding minerals) as compared to the CL-2D material (Tables 4, 5, and 6 of Part I).

Kinetics of Fe Solubility

Total Fe concentrations in the effluents of CL-1A and BD-1C decreased sharply the 8th and 14th day of leaching, respectively, probably as a result of prevailing reducing conditions in the column (Fig. 14). These concentrations dropped below the original Fe levels after the 20th day of the experiment as a result of dramatic pH increases. Abrupt Fe fluctuations at certain time periods in the effluents of OH-4D and BD-3A are attributed to alternating reducing and oxidizing environments, following the pattern of alternating wetting and drying cycles. The above interpretations were supported by the generally poor correlations of Fe with pH and SO_4^{2-} observed for OH-4D and CL-2D samples.

Iron (Fe^{3+}) solubility in the effluents of all but the two soil materials (BD-1C and CL-1A) fluctuated between that of jarosite and amorphous $Fe(OH)_3$ (Fig. 15). There was a cycling pattern between these two minerals for Fe^{3+} solubility control during which partial precipitation of one or the other may have occurred. The clustering of many points around the goethite saturation line suggests that this mineral may have also been involved in the control cycle.

Iron (Fe^{3+}) activities in the BD-1C effluent, after an initial undersaturation period consistent with the solubility of jarosite, approached gradually the amorphous Fe $(OH)_3$ solubility line along which they clustered during the rest of the experiment. The solubility of amorphous Fe $(OH)_3$ appeared to also control Fe^{3+} activities in the CL-1A effluents throughout the

experiment, with only some points, representing the final leaching stages, moving towards goethite solubility control (Fig. 15). As it was the case with Al the kinetics of Fe solubility did not appear to be influenced by the different leaching rates.

CONCLUSIONS

The column leaching experiments also confirmed that the major components controlling the behavior of these systems over time are primarily pH, SO_4^{2-}, Al and Fe. Alternating wetting and drying cycles appeared to cause more drastic changes in the above components than different flow rates. Two of the studied materials exhibited pH increases from 5.0 to 8.0 and from 3.0 to 5.5, respectively, within the first 30 days of leaching. These changes caused dramatic decreases in soluble Al levels. In most cases, however, these Al levels were maintained under the solubility control of Al-sulfate minerals. Two materials remained within the solubility range of jurbanite, two shifted from the jurbanite to the alunite range, and two from jurbanite to that of microcrystalline gibbsite. Iron release appears to follow a cycling pattern during which the solubility control of Fe in the effluent is alternating between jarosite, amorphous Fe $(OH)_3$ and goethite. These findings suggest that equilibrium relationships, although quite useful, may not be sufficient for predicting the dynamic behavior of systems such as those included in this study. Kinetic relationships reflecting Al and Fe released as a function of time and the sequence of mineral phases controlling Al and Fe solubility are also necessary in order to obtain more realistic models of Al and Fe release into aquifers of such systems.

REFERENCES

Adams, Fred. 1971. Ionic concentrations and activities in soil
solutions. Soil Sci. Soc. Am. Proc. 35:420-426.

Adams, Fred, and B.F. Hajek. 1978. Effects of solution sulfate
hydroxide and potassium concentrations on the crystallization of
alunite, basaluminite, and gibbsite from dilute aluminum
solutions. Soil Sci. 126:169-173.

American Public Health Association. 1976. Standard methods for the
examination of water and wastewater. 13th ed. U.S. Government
Printing Office, Washington, D.C.

Anthony, J.W., and W.J. McLean. 1976. Jurbanite, a new post-mine
aluminum sulfate mineral from San Manuel Arizona. Am. Miner.
61:1-4.

Caruccio, F.T., and G. Geidel. 1978. Geochemical factors affecting
coal mine drainage quality. In F.W. Schaller and P.Sutton (ed.)
Reclamation of drastically Disturbed Lands. Amer. Soc. Agron.,
Madison, WI.

Driscoll, C.T., J.P. Baker, J.J. Bisogni, and C.L. Schofield. 1984.
Aluminum speciation and equilibria in dilute acidic surface waters
of the Adirondalk region of New York State. In O.R. Bricker
(ed.), Acid Precipitation: Geological Aspects, Ann Arbor Sci.,
Ann Arbor, MI, pp. 55-75.

Evangelou, V.P., and A.D. Karathanasis. 1984. Reactions and mechanisms
controlling water quality in surface-mined spoils. pp. 213-247.
Symposium on the reclamation of lands disturbed by surface mining.
Am. Soc. Surf. Min. Recl., Owensboro, Kentucky. July 10-13, 1984.

Hall, F.R. 1970. Dissolved solute-discharge relationships: mixing
models. Water Resour. Res. 6:845-850.

Harmsen, K., and N. Van Breemen. 1975. Translocation of iron in acid
sulfate soils: II. Production and diffusion of dissolved ferrous
iron. Soil Sci. Soc. Am. Proc. 39:1148-1157.

Johnson, N.M., G. Likens, F.H. Bormann, D.W. Fisher and R.S. Pierce.
1969. A working model for the variation in stream water chemistry
at the Hubbard Brooks Experimental Forest, New Hampshire. Water
Resour. Res. 5:1353-1363.

Karathanasis, A.D., and B.F. Hajek. 1982. Revised methods for rapid quantitative determination of minerals in soil clays. Soil Sci. Soc. Am. J. 46:419-425.

Karathanasis, A.D., V.P. Evangelou and Y.L. Thompson. 1988. Aluminum and iron equilibria in soil solutions and surface waters of acid mine watersheds. Journ. Envir. Qual. 17:(in press).

Lewis, W.M. and M.C. Grant. 1979. Relationships between stream discharge and yield of dissolved substances from a Colorado mountain watershed. Soil Sci. 128:353-363.

Lindsay, W.L. 1979. Chemical equilibria in soils. John Wiley & Sons, Inc., New York.

Longbein, W.B. and D.R. Dowdy. 1964. Occurrance of dissolved solids in surface waters in the United States. U.S. Geol. Surv. Prof. Pap. 501-D, pp. 115-117.

Lowry, G.L. and J.H. Finney. 1962. A lysimeter for studying the physical and chemical changes in weathering coal spoils. Ohio Agric. Exp. Stn. Res. Circular 113, Wooster, Ohio.

Nordstrom, D.K. 1982. The effect of sulfate on aluminum concentrations in natural waters: Some stability relations in the system Al_2O_3-SO_4-H_2O at $298^{\circ}K$. Geochim, Cosmochim. Acta. 46:681-692.

Nordstrom, D.K., and J.W. Ball. 1986. The geochemical behavior of aluminum in acidified surface waters. Sci. 232:54-56.

Nordstrom, D.K., E.A. Jenne, and J.W. Ball. 1979. Redox equilbria of iron in acid mine waters: In E.A. Jenne (ed.) Chemical Modeling in Aqueous Systems, Speciation, Sorption, Solubility and Kinetics. Am. Chem. Soc. Symp. Ser. 93, p. 51-79.

Rodriguez-Clemente, R., and Hidalgo-Lopez, A. 1985. Physical conditions in alunite precipitation as a secondary mineral. In J. I. Drever (ed.) The chemistry of weathering, p. 121-141, Reidel Publishing Company.

Rogowski, A.S., H.B. Pionke, and J.G. Broyan. 1977. Modeling the impact of strip mining and reclamation processes on quality and quantity of water in mined areas: A review. J. Env. Qual. 6:237-244.

Singer, P.C. and W. Stumm. 1968. Kinetics of the oxidation of ferrous iron. p. 12-34. In Proc. 2nd Symp. on Coal Mine Drain Res. Pittsburg, PA 14-15 May, 1968. Coal Industry Advisory Comm. & Ohio River Valley Sanitation Commission.

Van Breemen, N. 1973. Dissolved aluminum in acid sulfate soils and in acid mine waters. Soil Sci. Soc. Am. Proc. 27:694-697.

Vimmerstedt, J.P. and P.H. Struthers. 1968. Influence of time and precipitation on chemical composition of spoil drainage. p. 152-163. In Proc.

LIST OF TABLES

50

Table 1: Ion activities (negative logs) in effluent solutions, of the BD-3A spoil material as a function of time.

Date	Rate(ml)	pH	pSO_4^{2-}	pCa^{2+}	pMg^{2+}	pK^+	pNa^+	pAl^{3+}	pMn^{2+}	pFe^{3+}
6-25	1	3.46	2.24	2.88	2.70	2.90	2.48	3.82	4.28	6.42
7-2	1	3.75	2.54	3.13	3.11	2.99	2.91	4.02	4.68	6.12
7-8	1	3.75	2.61	3.31	2.99	3.09	3.07	4.16	4.86	6.58
7-17	1	3.89	2.73	3.49	3.23	3.08	3.22	4.10	4.90	5.56
7-27	1	3.75	2.97	3.70	3.72	3.16	3.51	4.00	5.20	6.07
7-31	1	3.88	3.15	3.84	4.10	3.20	3.66	4.28	5.45	6.45
8-12	1	3.65	3.19	3.82	4.09	3.24	3.61	4.53	5.39	5.35
8-14	1	4.16	3.22	3.85	4.16	3.25	3.64	4.69	5.65	6.40
8-20	1	3.98	3.21	3.86	4.62	3.23	4.27	4.17	5.83	6.61
8-27	1	3.93	3.25	4.01	4.74	3.32	3.82	4.16	5.82	6.49
9-21	1	3.96	3.35	4.07	4.34	3.36	4.03	4.44	5.51	5.52
9-28	1	4.19	3.29	4.08	4.15	3.32	3.68	4.62		5.88
10-1	1	3.80	3.24	4.13	4.30	3.32	3.74	4.18	5.40	6.04
10-5	1	3.93	3.16	4.16	4.29	3.33	3.70	3.96	5.54	6.51
10-8	1	3.97	3.17	4.17	4.34	3.35	3.70	3.97	5.54	6.82
10-12	1	3.88	3.22	4.20	4.43	3.36	3.74	4.01	5.66	6.82
10-15	1	3.75	3.23	4.34	4.56	3.41	3.79	3.94	5.65	6.77
10-19	1	3.84	3.30	4.36	5.52	3.44	3.91	4.00	5.69	6.98
10-22	1	3.80	3.32	4.52	5.77	3.50	4.02	3.95	5.76	6.89
10-26	1	3.78	3.33	4.61	5.93	3.52	4.04	3.94	5.81	6.85
10-29	1	3.75	3.34	4.68	5.93	3.55	4.04	3.94	6.03	6.86
11-2	1	3.75	3.36	4.77		3.56	4.08	3.95	5.97	6.89
11-5	1	3.79	3.37	4.73	5.96	3.57	4.10	3.96	6.03	7.06
11-9	1	3.78	3.39	4.77	5.93	3.59	4.13	3.97	6.03	7.08
11-13	1	3.76	3.41	4.78	5.87	3.61	4.13	3.99	6.26	6.82
11-17	1	3.78	3.41	4.30	5.59	3.57	4.06	4.10	6.02	6.35
11-23	1	3.92	3.28	3.62	4.89	3.58	4.02	4.32	5.82	5.85

Table 1a: Ion activities (negative logs) in effluent solutions of the BD-3A spoil material as a function of time.

Date	Rate(ml)	pH	pSO$_4^{2-}$	pCa^{2+}	pMg^{2+}	pK$^+$	pNa$^+$	pAl^{3+}	pMn^{2+}	pFe^{3+}
6-25	3	3.58	2.33	2.93	2.82	2.97	2.61	3.87	4.38	6.67
6-26	3	3.73	2.66	3.25	3.21	3.07	3.13	4.08	4.72	8.20
6-30	3	3.80	3.14	3.69	4.06	3.24	3.82	4.28	5.40	8.22
7-2	3	3.83	3.27	4.08	5.89	3.36	4.24	4.01	6.12	8.32
7-8	3	3.79	3.33	4.04	5.28	3.43	4.08	4.13	6.16	6.62
7-10	3	3.75	3.38	4.31	5.64	3.46	4.10	4.11	5.26	7.09
7-13	3	3.74	3.38	4.46	5.87	3.50	4.15	4.02	6.41	6.97
7-15	3	3.58	3.29	4.69	6.20	3.58	4.15	3.83	5.98	7.14
7-17	3	3.65	3.29	4.82	6.49	3.61	4.24	3.81	6.05	7.50
8-12	3	4.15	3.44	4.54	5.33	3.44	3.76	4.45	5.44	5.88
8-14	3	4.09	3.35	4.66	4.55	3.44	3.74	4.20		6.34
9-18	3	4.02	3.36	4.60	4.71	3.43	3.74	4.21	5.50	6.27
9-21	3	3.96	3.39	4.73	5.18	3.50	4.02	4.07	5.64	6.61
9-28	3	3.87	3.47	4.84	5.73	3.56	4.10	4.14	5.95	6.44
10-1	3	3.79	3.47	5.06	6.30	3.62	4.28	4.04	6.14	6.84
10-5	3	3.83	3.51	5.09	6.23	3.70	4.35	4.07	6.14	7.28
10-8	3	3.83	3.55	5.01	6.29	3.74	4.38	4.11	6.13	7.52
10-12	3	3.87	3.58	5.17	6.32	3.76	4.39	4.13	6.13	7.69
10-15	3	3.79	3.67	5.16	6.24	3.78	4.39	4.26	6.07	7.66
10-19	3	3.80	3.60	5.32	6.41	3.76	4.45	4.14	6.08	7.90
10-22	3	3.82	3.59	4.80	6.28	3.76	4.36	4.18	6.00	8.10
10-26	3	3.77	3.61	5.29	7.16	3.78	4.47	4.14	6.08	7.91
10-29	3	3.74	3.61	5.36	6.38	3.78	4.46	4.14	6.08	7.80
11-2	3	3.75	3.60	5.38		3.76	4.48	4.14	6.08	7.99
11-5	3	3.78	3.59	5.22	6.16	3.74	4.42	4.14	6.08	8.60
11-9	3	3.76	3.63	5.16	6.07	3.76	4.42	4.20	6.00	8.34
11-13	3	3.94	3.60	4.57	5.73	3.78	4.41	4.23	6.12	7.98
11-17	3	3.82	3.58	4.43	5.96	3.76	4.43	4.22	6.38	7.99
11-23	3	3.84	3.60	4.40	5.87	3.81	4.54	4.22	6.38	8.13

52

Table 2: Ion activities (negative logs) in effluent solutions of the OH-4D spoil material as a function of time.

Date	Rate(ml)	pH	pSO_4^{2-}	pCa^{2+}	pMg^{2+}	pK^+	pNa^+	pAl^{3+}	pMn^{2+}	pFe^{3+}
6-25	1	2.27	1.72	2.55	2.28	5.79	4.13	3.01	3.93	5.37
7-2	1	2.46	2.02	2.35	2.82	5.64	4.47	3.42	4.51	5.71
7-8	1	2.63	2.11	2.36	3.03	5.60	4.42	3.54	4.69	5.70
7-17	1	2.56	2.14	2.32	3.01	4.94	4.32	3.68	4.77	5.22
7-27	1	2.56	2.16	2.30	3.19	4.81	4.42	3.76	5.06	5.31
7-31	1	2.72	2.17	2.32	3.34	4.63	4.41	3.71	5.36	5.23
8-12	1	2.64	2.12	2.26	3.37	4.31	4.16	3.68		5.27
8-14	1	2.76	2.16	2.30	3.42	4.47	4.22	3.71	5.36	4.91
8-20	1	2.79	2.18	2.29	3.48	4.51	4.31	3.79	5.35	5.05
8-27	1	2.89	2.36	2.56	3.65	4.68	4.42	3.73	5.29	5.07
9-13	1	2.84	2.23	2.31	3.85	4.84	4.47	3.89	5.55	5.70
9-21	1	2.97	2.22	2.31	3.96	4.54	4.51	3.88	5.55	6.02
9-25	1	2.93	2.24	2.30	4.22	4.60	4.52	3.94	5.72	5.99
9-28	1	2.97	2.26	2.35	4.01	4.66	4.59	3.88	5.84	5.54
10-1	1	2.93	2.25	2.31	4.51	4.75	4.72	3.96	6.02	6.05
10-5	1	2.99	2.26	2.34	4.35	4.84	4.67	3.91	6.02	5.58
10-8	1	2.96	2.22	2.28	4.34	4.42	4.30	3.93	6.03	5.61
10-12	1	3.00	2.26	2.33	4.55	4.75	4.61	3.92	6.32	6.01
10-15	1	2.97	2.27	2.34	4.66	4.77	4.59	3.94	6.31	6.02
10-19	1	2.95	2.26	2.29	4.87	4.84	4.69	4.11	6.32	5.99
10-22	1	2.97	2.26	2.30	4.96	4.79	4.64	4.05	6.32	5.95
10-26	1	2.93	2.26	2.30	5.01	4.68	4.59	4.07	6.31	5.82
10-29	1	2.97	2.26	2.29	4.83	4.56	4.45	4.08	6.02	5.71
11-2	1	2.97	2.25	2.29	4.62	4.48	4.39	4.08	6.32	5.69
11-9	1	3.02	2.27	2.31	4.87	4.67	4.54	4.08	6.31	5.68
11-13	1	3.04	2.25	2.27	4.97	4.79	4.58	4.17	6.36	5.90
11-17	1	2.98	2.52	2.66	5.04	4.72	4.54	3.89	6.28	6.11
11-23	1	2.95	2.25	2.27	5.21	4.92	4.64	4.15	6.37	6.31

Table 2a: Ion activities (negative logs) in effluent solutions of the OH-4D spoil material as a function of time.

Date	Rate(ml)	pH	pSO_4^{2-}	pCa^{2+}	pMg^{2+}	pK^+	pNa^+	pAl^{3+}	pMn^{2+}	pFe^{3+}
6-25	3	2.28	1.75	2.51	2.52	5.79	4.13	3.01	3.93	5.37
6-26	3	2.45	2.00	2.34	2.75	5.69	4.52	3.41	4.48	5.78
7-2	3	2.54	2.07	2.17	3.17	5.12	4.81	3.76	4.92	6.17
7-8	3	2.76	2.20	2.30	3.45	5.27	4.79	3.82	5.34	6.39
7-10	3	2.79	2.21	2.29	3.69	5.54	4.98	3.90	5.47	6.52
7-13	3	2.85	2.22	2.28	3.76	6.84	4.97	3.97	5.58	6.85
7-15	3	2.78	2.24	2.29	3.64	6.84	5.04	4.04	5.65	6.50
7-17	3	2.84	2.23	2.26	3.72	6.09	5.13	4.09	5.75	6.70
8-12	3	3.22	2.23	2.24	3.91	4.10	3.72	4.31		4.11
8-14	3	3.44	2.24	2.25	3.64	4.19	4.21	4.61	5.72	4.52
9-21	3	3.35	2.28	2.29	3.96	4.13	3.93	4.40	5.65	4.94
9-25	3	3.37	2.28	2.28	4.02	4.26	4.30	4.45	5.73	5.33

Table 3: Ion activities (negative logs) in effluent solutions of the OH-1E sediment material as a function of time.

Date	Rate(ml)	pH	pSO_4^{2-}	pCa^{2+}	pMg^{2+}	pK^+	pNa^+	pAl^{3+}	pMn^{2+}	pFe^{3+}
7-2	1	2.66	1.79	2.63	1.91	3.37	2.84	3.49	2.76	5.58
7-8	1	2.75	2.23	3.06	2.56	3.62	3.43	3.72	3.07	4.97
7-17	1	2.80	2.31	2.99	2.56	3.65	3.63	3.99	3.30	5.45
7-27	1	2.74	2.41	3.05	2.69	3.64	3.79	4.09	3.34	5.11
7-31	1	2.75	2.59	3.26	2.86	3.68	4.09	4.27	3.52	5.33
8-14	1	2.88	2.94	3.46	3.41	3.70	4.44	4.29	3.70	5.39
8-20	1	3.00	2.84	3.42	3.12	3.74	4.52	4.59	3.88	5.56
8-27	1	3.05	2.79	3.47	3.17	3.74	4.61	4.05	3.94	5.86
9-25	1	3.05	3.00	3.52	3.39	3.78	4.71	4.30	3.96	5.49
9-28	1	2.99	2.95	3.53	3.23	3.72	4.59	4.62	3.95	5.65
10-1	1	3.03	2.94	3.63	3.16	3.74	4.62	4.63	3.97	5.36
10-5	1	3.10	3.00	3.62	3.29	3.78	4.75	4.55	3.95	5.66
10-8	1	3.06	2.99	3.67	3.24	3.81	4.65	4.59	4.01	5.75
10-12	1	3.13	2.98	3.69	3.29	3.81	4.45	4.16	4.08	5.86
	1	3.11	3.08	3.73	3.33	3.83	4.61	4.68	4.12	5.96
	1	3.03	3.10	3.76	3.36	3.83	4.60	4.72	4.16	6.03
10-19	1	3.11	3.16	3.72	3.48	3.85	4.79	4.71	4.15	6.01
10-22	1	3.09	3.22	3.76	3.58	3.85	4.79	4.78	4.18	6.08
10-26	1	3.12	3.30	3.76	3.72	3.88	4.79	5.20	4.22	6.15
10-29	1	3.10	3.34	3.77	3.81	3.85	4.81	5.25	4.21	6.15
11-2	1	3.10	3.24	3.81	3.53	3.85	4.79	5.27	4.23	6.18
11-5	1	3.15	3.19	3.74	3.51	3.85	4.41	4.90	4.24	6.24
11-9	1	3.19	3.24	3.77	3.53	3.91	4.64	5.11	4.34	6.22
11-13	1	3.16	3.25	3.79	3.54	3.91	4.61	5.07	4.36	6.26
11-23	1	3.06	3.26	3.83	3.55	3.88	4.61	5.06	4.39	6.12

Table 3a: Ion activities (negative logs) in effluent solutions of the OH-1E sediment material as a function of time.

Date	Rate(ml)	pH	pSO_4^{2-}	pCa^{2+}	pMg^{2+}	pK^+	pNa^+	pAl^{3+}	pMn^{2+}	pFe^{3+}
6-25	3	2.60	1.90	2.48	2.46	3.40	3.00	3.38	2.71	5.44
6-30	3	2.75	2.10	2.69	2.46	3.61	3.38	3.69	3.02	5.32
7-6	3	2.76	2.36	2.88	2.77	3.62	3.38	3.84	3.78	5.33
7-8	3	2.98	2.46	3.12	2.73	3.71	3.70	4.10	3.43	5.35
7-10	3	2.95	2.55	3.17	2.79	3.74	4.02	4.16	3.99	5.46
7-13	3	2.90	2.55	3.21	2.83	3.70	4.06	4.20	3.51	5.48
7-15	3	2.83	2.63	3.26	2.91	3.71	4.21	4.27	3.56	5.40
7-17	3	2.86	2.66	3.29	2.94	3.73	4.27	4.31	3.57	5.41
7-27	3	2.77	2.70	3.34	2.98	3.73	4.35	4.39	3.63	5.94
8-14	3	3.01	2.83	3.43	3.11	3.76	4.56	4.50	3.86	5.18
8-17	3	3.04	2.82	3.40	3.11	3.76	4.56	4.50	3.86	5.74
9-21	3	3.23	2.99	3.60	3.26	3.78	4.55	4.66	3.98	4.95

Table 4: Ion activities (negative logs) in effluent solutions of the CL-2D sediment material as a function of time.

Date	Rate(ml)	pH	pSO_4^{2-}	pCa^{2+}	pMg^{2+}	pK^+	pNa^+	pAl^{3+}	pMn^{2+}	pFe^{3+}
6-25	1	2.83	2.32	3.00	2.67	3.97	3.82	3.72	3.55	6.37
7-2	1	2.92	2.55	3.16	2.88	3.98	4.35	4.03	3.57	5.51
7-8	1	3.06	2.68	3.35	2.88	4.17	4.57	4.36	3.89	5.16
7-17	1	2.85	2.72	3.51	2.99	3.97	4.45	4.14	3.74	5.28
7-27	1	2.90	2.98	3.75	3.24	4.04	4.56	4.16	4.05	5.48
7-31	1	2.98	3.03	3.78	3.32	3.59	4.40	4.42	4.06	5.36
8-12	1	2.85	2.98	3.66	3.29	3.53	4.32	4.36	4.04	5.36
8-14	1	3.19	3.04	3.66	3.35	3.62	4.40	4.49	4.24	5.39
8-20	1	3.15	3.05	3.73	3.60	3.69	4.40	3.92	4.34	5.82
8-27	1	3.20	3.23	3.81	3.62	3.75	4.45	4.55	4.31	6.28
9-18	1	3.18	3.12	3.78	3.41	3.71	4.44	4.57	4.30	5.31
9-21	1	3.19	3.18	3.86	3.48	3.75	4.49	4.55	4.36	5.69
9-25	1	3.17	3.24	3.83	3.62	3.72	4.49	4.64	4.29	5.67
9-28	1	3.23	3.20	3.96	3.47	3.77	4.52	4.69	4.29	5.69
10-1	1	3.22	3.40	3.90	3.95	3.82	4.64	4.65	4.41	6.20
10-5	1	3.24	3.23	3.83	3.53	3.82	4.59	4.74	4.43	6.36
10-8	1	3.26	3.27	3.90	3.54	4.08	4.56	4.72	4.43	6.51
10-12	1	3.26	3.23	3.79	3.56	3.80	4.53	4.78	4.43	6.49
10-15	1	3.19	3.13	3.87	3.57	3.77	3.31	4.79	4.45	6.50
10-19	1	3.18	3.39	4.03	3.85	3.77	4.53	4.63	4.41	6.45
10-22	1	3.20	3.35	3.88	3.88	3.72	4.53	4.67	4.41	6.66
10-26	1	3.17	3.35	3.86	3.88	3.72	4.49	4.66	4.41	6.41
10-29	1	3.10	3.31	3.84	3.79	3.70	4.46	4.69	4.42	6.31
11-2	1	3.13	3.32	3.89	3.79	3.70	4.46	4.67	4.42	6.35
11-5	1	3.18	3.30	4.01	3.64	3.72	4.39	4.69	4.42	6.29
11-9	1	3.23	3.31	4.00	3.65	3.74	4.49	4.78	4.42	6.16
11-13	1	3.25	3.34	3.81	3.77	3.77	4.54	4.89	4.67	6.26
11-17	1	3.24	3.48	4.55	3.79	3.74	4.55	4.82	4.68	6.48
11-23	1	3.17	3.44	4.13	3.82	3.74	4.60	4.87	4.72	6.37

57

Table 4a: Ion activities (negative logs) in effluent solutions of the CL-2D sediment material as a function of time.

Date	Rate(ml)	pH	pSO_4^{2-}	pCa^{2+}	pMg^{2+}	pK^+	pNa^+	pAl^{3+}	pMn^{2+}	pFe^{3+}
6-25	3	2.78	2.34	2.99	2.72	3.94	4.00	3.73	3.56	6.19
6-26	3	2.96	2.85	3.37	3.28	4.00	4.70	4.17	3.90	5.83
6-30	3	3.14	3.10	3.52	3.43	4.17	5.19	4.67	4.38	6.47
7-2	3	3.23	3.46	4.02	3.75	4.16	5.12	4.97	4.68	6.23
7-8	3	3.23	3.38	3.99	3.67	3.94	4.68	4.88	4.63	5.28
7-10	3	3.28	3.43	4.02	3.73	3.94	4.79	5.07	4.69	5.47
7-13	3	3.22	3.45	4.06	3.75	3.98	4.79	4.97	4.80	5.55
7-15	3	3.14	3.45	4.11	3.75	3.94	4.79	4.93	4.80	5.59
7-17	3	3.15	3.48	4.18	3.77	3.94	4.79	4.92	4.79	5.73
8-12	3	2.96	3.12	3.83	3.55	3.40	4.03	4.74	4.04	4.54
8-14	3	3.52	3.35	3.83	4.03	3.53	4.27	5.02	4.43	5.10
9-18	3	3.29	3.16	3.84	3.59	3.39	4.14	4.76	4.27	4.63

Table 5:   Ion activities (negative logs) in effluent solutions of the BD-1C soil material as a function of time.

Date	Rate(ml)	pH	pSO_4^{2-}	pCa^{2+}	pMg^{2+}	pK^+	pNa^+	pAl^{3+}	pMn^{2+}	pFe^{3+}
6-25	1	2.93	2.33	2.94	2.99	3.50	3.26	3.59	3.53	5.60
7-2	1	3.08	2.53	3.08	3.04	3.57	3.95	3.88	3.58	4.49
7-8	1	3.34	2.72	3.25	3.02	3.62	4.30	4.46	3.75	4.32
7-17	1	2.66	2.99	3.54	3.31	3.71	4.55	4.52	3.98	4.48
7-27	1	3.22	3.17	3.80	3.49	3.80	4.91	4.49	4.24	5.19
7-31	1	3.52	3.48	3.80	3.79	3.84	4.90	4.57	4.32	7.24
8-14	1	5.24	3.40	3.81	3.78	4.08	4.81	6.80	4.33	8.07
8-20	1	4.88								
8-27	1	5.38	3.43	3.99	3.74	4.13	5.02	6.60	4.36	8.47
9-18	1	5.35	3.56	3.88	4.04	4.18	4.94	7.49	4.34	8.35
9-21	1	5.16	3.57	4.04	3.88	4.30	5.03	6.81	4.61	7.93
9-25	1	5.54	3.81	4.22	4.11	4.26	4.93	7.70	4.76	9.06

Table 5a: Ion activities (negative logs) in effluent solutions of the BD-1C soil material as a function of time.

Date	Rate(ml)	pH	pSO_4^{2-}	pCa^{2+}	pMg^{2+}	pK^+	pNa^+	pAl^{3+}	pMn^{2+}	pFe^{3+}
6-25	3	2.84	2.43	2.98	3.05	3.45	3.45	3.73	3.55	5.20
6-26	3	3.79	2.96	3.38	3.67	3.61	4.44	4.06	3.92	4.80
6-30	3	3.54	3.17	3.68	3.55	3.82	4.98	4.53	4.23	4.89
7-2	3	3.66	3.38	3.85	3.76	3.94	5.20	5.10	4.44	5.24
7-8	3	4.91	3.49	3.95	3.88	4.03	5.08	6.36	4.50	7.36
7-10	3	4.94	3.51	3.94	3.91	4.03	5.08	6.41	4.51	7.49
7-13	3	5.25	3.54	3.97	3.94	4.05	5.38	6.99	4.53	8.18
7-15	3	4.51	3.55	4.01	3.91	4.15	5.42	5.90	4.61	6.87
7-17	3	4.94	3.61	4.12	3.96	4.16	5.54	6.30	4.60	7.67
8-14	3	5.20	3.34	3.78	3.61	4.44	4.87	6.90	4.20	7.59
8-17	3	5.32	3.73	4.07	4.17	4.60	4.97	7.43	4.54	8.13
8-18	3	4.65	3.77	4.28	4.19	4.40	4.93	5.92	4.66	6.99

Table 6: Ion activities (negative logs) in effluent solutions of the CL-1A soil material as a function of time.

Date	Rate(ml)	pH	pSO_4^{2-}	pCa^{2+}	pMg^{2+}	pK^+	pNa^+	pAl^{3+}	pMn^{2+}	pFe^{3+}
6-25	1	4.82	2.06	2.09	2.85	2.95	3.60	6.15	3.99	8.30
7-2	1	3.91	2.28	2.34	3.19	3.24	3.80	6.24	3.68	5.33
7-8	1	7.74	3.27	2.88	3.55	3.39	3.95	13.16	4.19	14.04
7-13	1	8.41	5.12	3.49	4.10	3.57	4.16	15.70	4.65	16.95
7-17	1	8.15	5.72	3.48	4.16	3.62	4.23	14.64	4.64	16.41
7-27	1	7.91	6.18	3.32	4.03	3.55	4.32	13.80	4.48	15.74
7-31	1	8.05	6.84	3.34	4.02	3.58	4.36	14.51	4.60	15.80
8-12	1	7.98	5.51	3.02	3.75	3.40	4.06	14.27	4.51	15.97
8-14	1	7.85	6.26	2.87	3.63	3.42	4.03	13.86	4.14	15.64
8-20	1	7.97	5.83	2.93	3.56	3.35	3.82	14.23	4.99	15.44
8-27	1	7.89	6.05	3.19	3.58	3.36	4.03	14.66	5.60	15.18
8-31	1	7.97	5.69	3.19	3.85	3.44	4.03	13.79	4.77	14.24
9-25	1	8.50	7.33	3.86	4.12	3.42	4.19	16.34	7.52	17.24

61

Table 6a: Ion activities (negative logs) in effluent solutions of the CL-1A soil material as a function of time.

Date	Rate(ml)	pH	pSO_4^{2-}	pCa^{2+}	pMg^{2+}	pK^+	pNa^+	pAl^{3+}	pMn^{2+}	pFe^{3+}
6-25	3	4.50	2.10	2.12	2.97	3.16	3.64	6.13	3.81	6.58
6-26	3	4.36	2.49	2.56	3.36	3.45	4.06	5.88	3.94	6.19
7-2	3	4.98	2.61	2.70	3.49	3.49	4.16	6.43	4.12	7.63
7-8	3	7.71	3.37	2.90	3.61	3.45	4.14	13.23	4.29	14.03
7-10	3	7.64	3.56	3.07	3.79	3.49	4.21	13.00	4.36	14.30
7-13	3	7.92	3.99	3.26	3.89	3.48	4.26	13.93	4.53	15.64
7-15	3	7.83	3.84	3.05	3.72	3.47	4.10	13.63	4.41	15.46
7-17	3	8.02	3.98	3.10	3.76	3.47	4.12	14.18	4.35	15.89
7-27	3	8.11	4.17	3.20	3.86	3.48	4.13	14.50	4.48	16.51
8-12	3	8.13	5.03	3.30	3.69	3.29	3.77	14.67	5.03	15.45
8-14	3	8.29	5.34	3.38	3.87	3.40	3.85	15.55	4.29	16.75
9-14	3	7.88	4.84	3.40	3.79	3.37	3.89	13.55	5.95	15.50

Fig. 1

□ OH 4D
■ OH 1E
○ BD 3A
● BD 1C
☆ CL 1A
★ CL 2D

Time, Days

pH

64

Fig. 2

Legend:
- □ OH 4D
- ■ OH 1E
- ○ BD 3A
- ● BD 1C
- ★ CL 2D
- ☆ CL 1A

Y-axis: SO₄, mMoles (0, 6.0, 12.0, 18.0, 24.0, 30.0, 36.0)

X-axis: Time, Days (20, 40, 60, 80, 100, 120, 140)

Fig. 3

Legend:
- □ OH 4D
- ■ OH 1E
- ○ BD 3A
- ● BD 1C
- ★ CL 2D
- ☆ CL 1A

Y-axis: Al, mMoles

X-axis: Time, Days

66

Fig. 4

□ OH 4D
■ OH 1E
○ BD 3A
● BD 1C
☆ CL 1A
★ CL 2D

p Al3+

Time, Days

67

Fig. 5

Legend:
- □ OH 4D
- ■ OH 1E
- ○ BD 3A
- ● BD 1C
- ☆ CL 1A
- ★ CL 2D

mMoles Ca (vertical axis): 14.0, 10.0, 6.0, 2.0

Time, Days (horizontal axis): 20, 40, 60, 80, 100

68

Fig. 6

Legend:
- □ OH 4D
- ■ OH 1E
- ○ BD 3A
- ● BD 1C
- ☆ CL 1A
- ★ CL 2D

mMoles Mg

Time, Days

69

Fig. 7

70

Fig. 8

71

Fig. 9

Fig. 10

CL-1A

Microcrystalline Gibbsite

Basaluminite

Gibbsite

Kaolinite

Alunite

Jurbanite

● 1 ml / hour
○ 3 ml / hour

$2pH + pSO_4^{2-}$

$pAl^{3+} + 3pOH$

Fig. 11

BD-1C

Fig. 12

CL-2D

- ● 1 ml / hour
- ○ 3 ml / hour

Gibbsite

Kaolinite

Basaluminite

Alunite

Jurbanite

K-Aluminite

2 pH + pSO$_4$

pAl + 3pOH

Fig. 13

OH 1E

76

Fig. 14

Legend:
- □ OH 4D
- ■ OH 1E
- ○ BD 3A
- ● BD 1C
- ☆ CL 1A
- ★ CL 2D

Y-axis: Fe, mMoles

X-axis: Time, Days

Fig. 15

Legend:
- ○ OH 4D
- ● OH 1E
- □ CL 2D
- ■ CL 1A
- ★ BD 1C
- ▲ BD 3A

Y-axis: pFe^{3+}

X-axis: $2\,pH - \frac{2}{3}\,pSO_4^{2-}$

Goethite

Jarosite

Amorphous $Fe(OH)_3$